Journal of Volcanology and Geothermal Research 405 (2020) 107041

Contents lists available at ScienceDirect

Journal of Volcanology and Geothermal Research

journal homepage: www.elsevier.com/locate/jvolgeores

Distal tephra from Campanian eruptions in early Late Holocene fills of the Agro Pontino graben and Fondi basin (Southern Lazio, Italy)

Jan Sevink [a,*], Wouter van Gorp [b], Mauro A. Di Vito [c], Ilenia Arienzo [c]

[a] Institute for Biodiversity and Ecosystem Dynamics (IBED), University of Amsterdam, Sciencepark 904, 1098 XH Amsterdam, the Netherlands
[b] Groningen Institute of Archaeology, Poststraat 6, 9712 ER Groningen, the Netherlands
[c] Istituto Nazionale di Geofisica e Vulcanologia (INGV), Via Diocleziano 328, 80124 Napoli, NA, Italy

ARTICLE INFO

Article history:
Received 1 March 2020
Received in revised form 19 August 2020
Accepted 31 August 2020
Available online 7 September 2020

Keywords:
Distal tephra
Tephrochronology
Geochemistry
Radiocarbon dating
Early Late Holocene
Central Italy

ABSTRACT

Following on the discovery (in 2011) of a layer of distal tephra from the Pomici di Avellino eruption (Somma-Vesuvius, EU5) in the Agro Pontino (southern Lazio, Italy), further detailed study of the Holocene sediment archives in this graben and in the nearby Fondi coastal basin showed that distal tephra from this EU5 eruption occurs as a rather continuous, conspicuous layer. Two other, less conspicuous tephra layers were found, identified as the earlier Astroni 6 eruption from the Campi Flegrei (Fondi basin) and the later AP2 eruption of the Somma-Vesuvius (Agro Pontino). The identification of the distal tephra layers rests upon a combination of criteria, including stratigraphy, macro characteristics, mineralogy, geochemical data on glass composition, Sr-isotopic ratios, and the known tephrochronology for the period concerned, i.e. between c. 2500 and 1000 BCE. ^{14}C datings serve to constrain their age. No significant spatial variation in the characteristics of the main tephra layer (EU5) was observed, other than distinct fining with increasing distance from the vent. Based on a detailed palaeogeographical reconstruction, the occurrence and preservation of these tephra are explained by the local environmental conditions governing their preservation during this time span (the Central Italian Bronze Age), and by the later evolution of the area. The observations underpin that multiple corings are needed to fully assess whether sedimentary hiatuses exist in palaeorecords, based on cores from sediment archives. Lastly, our study shows that hazard evaluations for future eruptions by Campanian volcanoes should pay more attention to their potential impacts on distal areas.

1. Introduction

Systematic study of distal tephra from the final phreatomagmatic phase of the Vesuvian Pomici di Avellino eruption (EU5, Sulpizio et al., 2008, 2010a and 2010b) is one of the main topics of the Avellino Event project. This project started in 2015 and focusses on the Agro Pontino graben and nearby Fondi basin in southern Lazio (Fig. 1). It includes a detailed reconstruction of the contemporary Early Bronze Age landscape, based on a large set of corings, filling gaps in earlier coring data sets (Sevink et al., 1984; Van Joolen, 2003; Feiken, 2014), and on detailed study (tephrochronology, radiocarbon dating, palaeoecology) of specific sites (see Fig. 1 and Table 1).

In the interior low-lying part of the Agro Pontino, two major Holocene sedimentary complexes were distinguished (Sevink et al., 1984; van Gorp and Sevink, 2019; van Gorp et al., 2020): a coastal lagoonal system near Terracina with associated valley system of the Amaseno river and a large inland lake with associated fluvio-deltaic system. In both complexes, in hundreds of corings a several centimetres thick tephra layer was found with quite uniform conspicuous field characteristics. This was the only major tephra layer encountered in these complexes and had already been identified as distal EU5 tephra and ^{14}C-dated at two sites by Sevink et al. (2011). In subsequent years it was also described by Sevink et al. (2013), Feiken (2014) and Bakels et al. (2015). In the Fondi basin, a similar situation was encountered (van Gorp and Sevink, 2019) with an inland lake and a small frontal lagoon holding this tephra layer (see also Doorenbosch and Field, 2019; van Gorp and Sevink, 2019). Fig. 2 shows the overall geology and potential occurrence of the Avellino tephra layer, further referred to as the AV-layer.

The situation became more complex, when a second thinner tephra layer was found above the AV-layer in some corings in the south of the Agro Pontino, near Borgo Hermada. In the Fondi basin, the situation was also complex. At two sites double tephra layers were found of which the upper had the characteristics of the AV-layer and the lower, thinner and finer textured layer thus should predate the AV-eruption and have a non-Vesuvian origin (e.g. Santacroce et al., 2008; Zanchetta et al., 2011). This was not truly surprising in the light of the presence in the Maccarese lagoon, further north near Rome, of Mid-Holocene tephra

* Corresponding author.
E-mail addresses: j.sevink@uva.nl (J. Sevink), W.van.Gorp@rug.nl (W. van Gorp), mauro.divito@ingv.it (M.A. Di Vito), ilenia.arienzo@ingv.it (I. Arienzo).

https://doi.org/10.1016/j.jvolgeores.2020.107041

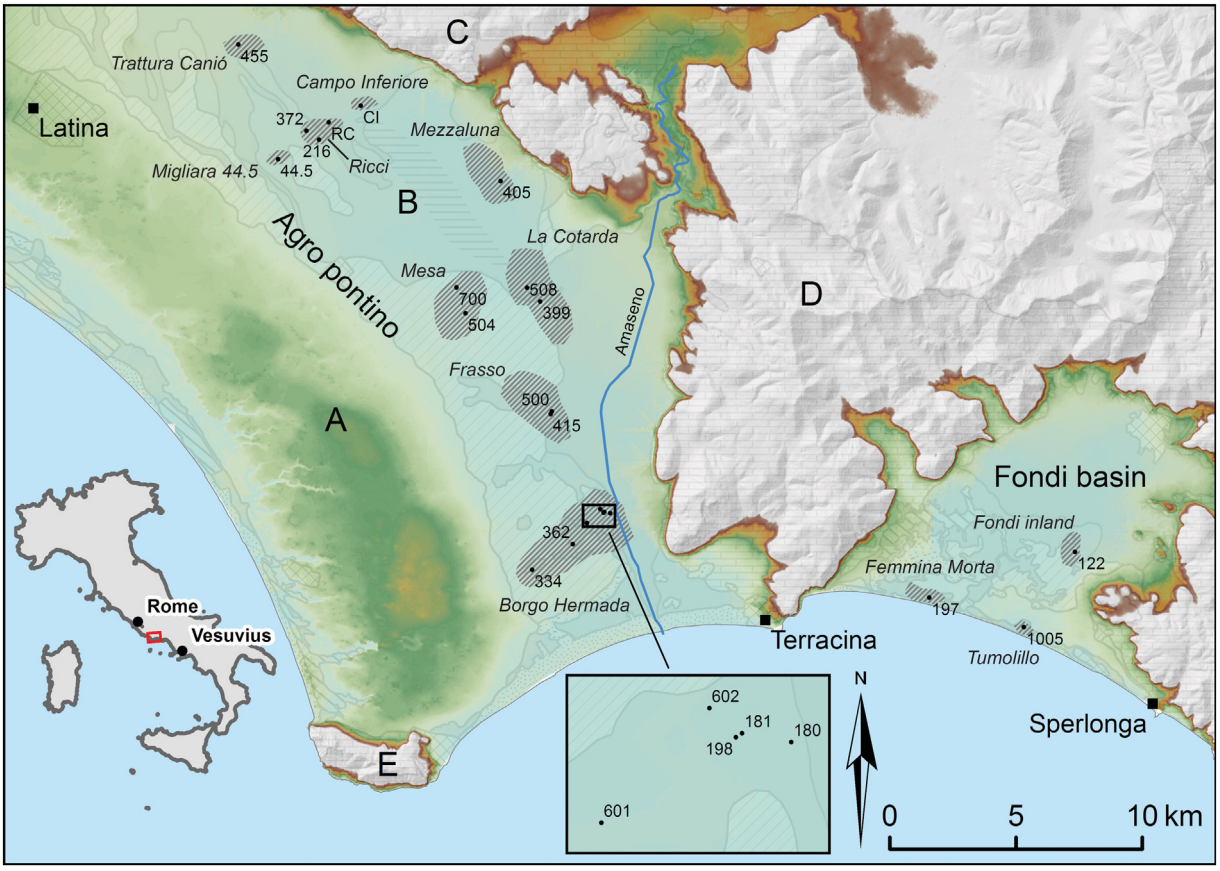

Fig. 1. Locations in the Agro Pontino and Fondi basin (shaded areas), and sites studied. Numbers refer to sites described in Table 1 (RC = site Ricci; CI = site Campo). A = higher complex of Pleistocene marine terraces; B = Agro Pontino graben; C = Monti Lepini; D = Monti Ausoni; E = Monte Circeo.

layers of Phlegraean origin (Jouannic et al., 2013), testifying to the distribution of distal tephra from Campi Flegrei eruptions far to the NW.

In this paper, we present a detailed overview of the geochemical and petrological characteristics of the AV-layer and its distribution in the two major coastal basins of Southern Lazio, and of the other distal tephra layers encountered. Results include a series of ^{14}C datings. We also describe the spatial variability in the occurrence and composition of the AV-layer and discuss the implications of our results for tephrostratigraphic studies of sediment cores from similar central Mediterranean environments. Lastly, we pay attention to hazards to which more remote distal areas may be exposed upon relatively minor eruptive events in the Campi Flegrei and Vesuvius areas (Orsi et al., 2009; Cioni et al., 2008). These are not accounted for in the current hazard evaluation and emergency plans (Sulpizio et al., 2014).

2. General information

During the last glacial period, with very low sea level, in the Agro Pontino and Fondi basin rivers cut deep valleys into a thick complex of predominantly fine-textured Quaternary sedimentary units (e.g. Sevink et al., 1984). Upon the Holocene sea level rise, these valleys gradually were filled in. Towards c. 2 ka BC, when sea level rise truly decreased (Lambeck et al., 2011; Vacchi et al., 2016), beach ridges could build up (Sevink et al., 1982, 1984, 2018; Van Gorp and Sevink, 2019; van Gorp et al., 2020). This created the low energy aquatic to semi-terrestrial environment that allowed for preservation of even thin distal tephra layers. Near the coast, these suited environments were mostly freshwater lagoons, which overall were shallow and underlain by sandy beach ridge deposits, while further inland the lagoons graded into marshy valleys. In the central part of the Agro Pontino basin a different situation existed. Upon sea level rise the Amaseno river built up an alluvial fan, which shortly before the AV-eruption started to block the single outlet of the fluvial system that drained the northern part of this basin, south of La Cotarda (Fig. 1). This led to a gradual 'drowning' of the earlier inland landscape and created a large lake and associated marshes (van Gorp and Sevink, 2019; van Gorp et al., 2020). In the NE part of this lake, peat with intercalated lacustrine marls (calcareous gyttja) and some travertine accumulated, whereas in the SW pyritic black organic clays were found. In the NW, these lacustrine deposits graded into fluvio-deltaic sediments and, further upstream, truly fluvial sediments. The waters that ran into the lake from the adjacent mountains were largely fed by springs with highly calcareous and often sulphuric waters.

The pattern in the Agro Pontino is depicted in Fig. 3 (after van Gorp and Sevink, 2019). A rather similar situation existed in the Fondi basin, where an inland lake formed with peats and calcareous gyttja. Large tracts of the Early Bronze Age landscape in both the Agro Pontino and the Fondi basin were later covered by mostly fine textured fluvial and colluvial deposits and by later peats (see Sevink et al., 1984; Van Joolen, 2003; Feiken, 2014). Thicknesses of this younger cover may be limited, in which case deep modern soil labour (often up to 50 cm and more) has obliterated any intercalated tephra layers.

Based on the foregoing, a fairly detailed picture could be constructed of the sedimentary complexes that potentially hold distal Early Bronze Age and later tephra layers. Truly earlier Holocene tephra layers are very unlikely to be found, with the possible exception of the deep fluvial incisions in which they potentially may occur, but in that case at great depths. The interior lake in the Agro Pontino most probably only formed shortly before the Bronze Age and for that reason is unlikely to hold earlier Holocene tephra layers (e.g. Sevink et al., 2018).

Table 1
General information on sites sampled and their main characteristics. Earlier studied sites are indicated in italics. Chem = Microprobe analyses; Micro = Thin sections; Text = Grain size analyses. AV = Avellino tephra. Facies: P = peat/peaty clay; A = anoxic, pyritic clay; G = calcareous gyttja; F = fluvio-deltaic sediment. For analyses: x = data available. ^{14}C: (x) = unreliable dating. Chem: (x) = no glass.

Locations	Sites (Fig. 1)	Name/nr	Coordinates site		Depth/thickness/nature tephra layer	Facies	Pollen	^{14}C	Chem	Micro	Text	Refer.
Agro Pontino												
Migliara 44.5	*44.5*	*44.5*	13.0139	41.4484	ca. 100 cm, 2 cm AV	A		x	x	x	x	
Campo inferiore	*Campo*	*Campo*	13.0525	41.4682	ca. 220 cm, 2 cm AV	G/F/P		x			x	Sevink et al., 2011
Mezzaluna	*405*	*405*	13.1195	41.4424	ca. 45 cm, 2–3 cm AV		x	x		x	x	
Ricci	*Ricci*	*Ricci*	13.0374	41.4620	ca. 210 cm, 2–3 cm AV	F	x	x				Bakels et al., 2015
Tratturo Caniò	*455*	*455*	12.9937	41.4890	ca. 150 cm, 2–3 cm AV	F		x			x	Feiken, 2014
	415	415	13.1456	41.3596	108 cm, 2 cm AV	P					x	
Frasso	500	500	13.1462	41.3605	ca. 55 cm, 2 cm AV	P	x	x		x		
	504	504	13.1046	41.3948	44 cm, 2 cm AV	A			(x)	x		
Mesa	700	700	13.0998	41.4040	46 cm, 2 cm AV	A		x				
	362	362	13.1575	41.3133	60 cm, 2 cm AV	P	x	x		x	x	
	601	601	13.1640	41.3209	60 cm, 2 cm AV	G	x	(x)				
Borgo Hermada	602	602	13.1701	41.3260	112 cm, 3 cm AV	G		x				
Fondi												
Femmina Morta	197	197-U	13.3266	41.2968	52 cm, 3 cm AV	P	x	x	x	x	x	Doorenbosch and Field, 2019
		197-L			66 cm, 2 cm lower tephra	P		x	x	x	x	
Tumolillo	1005	1005-U	13.3715	41.2869	88 cm, 2–3 cm AV	P	x	x	(x)			
		1005-L			112 cm, 2 cm lower tephra	P		x	x			
Fondi inland	122	122	13.3951	41.3141	81 cm, 2 cm AV	P	x	x	x			
Other												
	216	216	13.0331	41.4557	85 cm, 2 cm AV	A			(x)			
Ricci	372	372	13.0270	41.4588	105 cm, 2 cm AV	A					x	
	180	180-U	13.1749	41.3246	164 cm, 1 cm upper tephra	G			(x)			
	181	181-U	13.1720	41.3249	190 cm, 1 cm upper tephra	G			x			
	198	198-L	13.1717	41.3248	188 cm, 2 cm AV	G			x			
Borgo Hermada	334	334	13.1385	41.3038	149 cm, 2 cm AV	P					x	
	399	399	13.1396	41.3997	44 cm, 2 cm AV	A					x	
La Cotarda	508	508	13.1332	41.4045	70 cm, 2 cm AV	P					x	

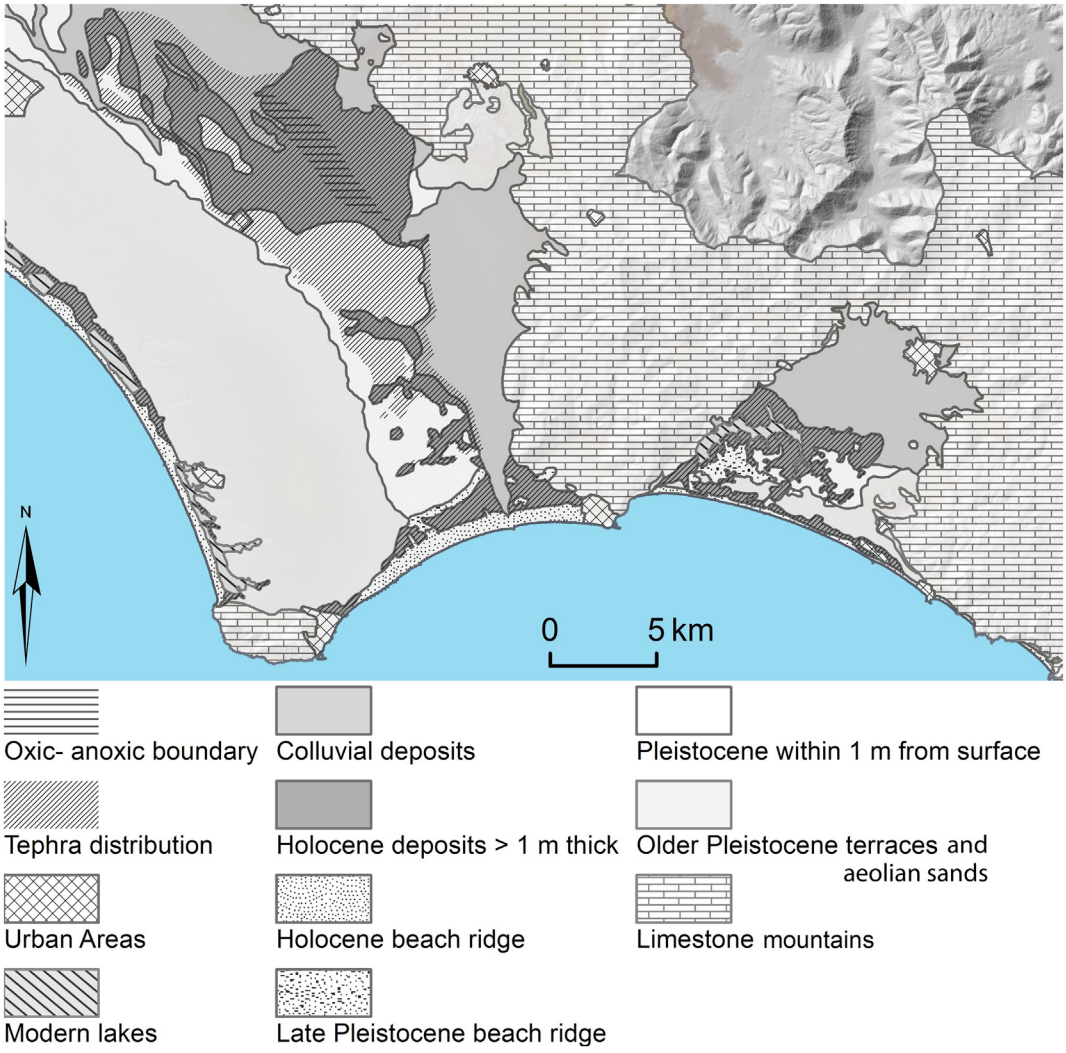

Fig. 2. Simplified geological map of the Agro Pontino and Fondi basin, also showing the potential tephra distribution (shaded areas), after Van Gorp and Sevink (2019).

3. Materials and methods

Basically, the identification of tephra layers encountered in the coastal basins studied and their origin hinges on five criteria: 1) field (macro) characteristics, 2) stratigraphy of the section concerned, 3) chemical composition (glass shards), 4) age constraints based on ^{14}C dating, and 5) isotopic composition (minerals and glass). Incidentally, archaeological dating can be used as an additional criterion for their age, notably at Tratturo Caniò and Ricci (Fig. 1), both with Early to Early Middle Bronze Age ceramics directly above the tephra layer (Feiken, 2014; Bakels et al., 2015). Methods described below pertain to the field criteria (1 and 2) and to the laboratory (3, 4, and 5). Analytical techniques are described in brief. Details are given as Supplemental information. Archaeological data have been published elsewhere and, where relevant, reference will be made to those publications.

3.1. Selection of sites and sampling

In the area indicated in Fig. 2 as potentially holding the AV-layer a large number of hand corings was carried out to assess the characteristics of the Holocene sedimentary fill, including the occurrence of tephra layers. Transitions from the Holocene unripe and often highly organic sediments, lacking any trace of soil formation, to the Pleistocene dense sediments with strong soil formation are very prominent and abrupt, allowing for easy distinction between these sediments (see e.g. van Gorp et al., 2020). Maximum depths reached by hand corings in the Holocene fills of the deeper river incisions were in the order of 10 m, often not touching the Pleistocene basis. Outside these incisions the thickness of the fill was generally limited to less than a few metres and its stratigraphy could be established in detail.

An important purpose of the coring program was to identify potential sites with well-preserved tephra layers that, together with already known and studied sites (e.g. Migliara 44.5 and Campo inferiore, Sevink et al., 2011), could provide a full picture of the tephra in the Agro Pontino graben and Fondi basin. Additional selection criteria were their suitability for palaeoecological studies and ^{14}C dating. Earlier studied and newly selected sites are indicated in Fig. 1 and listed in Table 1.

Sequences at newly selected sites were sampled with a six-centimetre diameter gauge corer (always multiple cores) or by taking a large monolith in a pit. Undisturbed samples were packed in plastic and stored in a cool environment till transport to the laboratory at Leiden, The Netherlands, where they were kept in a refrigerator or cold room.

3.2. Geochemical, petrological and geochronological analyses

Thin sections of undisturbed samples for microscopic study were produced at the RCE (Amersfoort, The Netherlands) by impregnation with resin, followed by cutting and polishing to a thickness of c.

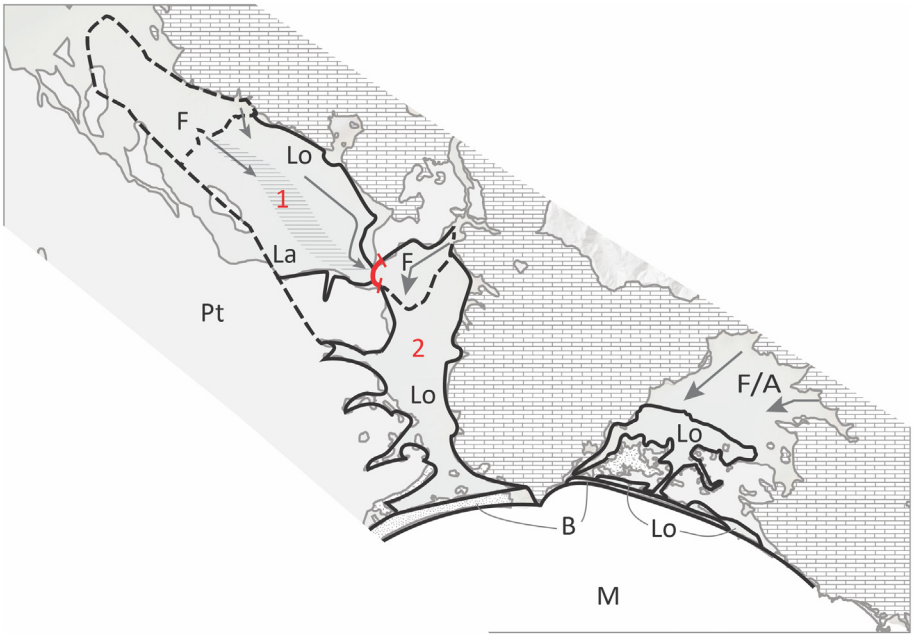

Fig. 3. Landscape Southern Lazio c. 2000 BCE. Agro Pontino: coastal lake (2) and inland lake (1), with oxic (Lo) and anoxic (La) lacustrine sediments, and shaded transitional zone; fluvio-deltaic sediments (F); Pleistocene deposits (Pt). Fondi basin: oxic lacustrine sediments (Lo); fluvio-deltaic and alluvial sediments (F/A). B = beach ridges. M = Mediterranean Sea. Arrows indicate former river courses. For details on Pleistocene deposits: see Fig. 2. Tentative boundary indicated with ———.

30 μm. Polished sections for microprobe analysis were produced by the GeoLab of the University of Utrecht (Utrecht, The Netherlands), using resin impregnated undisturbed samples or resin-embedded pumice fragments that were hand-picked from fractions >63 μm. These fractions were obtained by wet sieving, following on treatment with 5% H_2O_2 to remove organic matter and by 5% HCl to remove carbonates. Both thin sections and size fractions were studied using a petrographic microscope.

3.2.1. Chemical analyses

Microprobe analyses were performed at the HP-HT Laboratory of Experimental Volcanology and Geophysics of the Istituto Nazionale di Geofisica e Vulcanologia at Rome (Italy), using a Cameca SX50 electron microprobe equipped with five wavelength-dispersive spectrometers using 15 kV accelerating voltage, 15 nA beam current, 10 Am beam diameter, and 20 s counting time. In some cases, glass in thin sections was deeply altered and therefore not all samples were analysed.

3.2.2. Isotopic analyses

Sr isotopic compositions were determined on minerals >63 μm separated from the corresponding size fractions, pretreated as described above. The analyses concern a selection of tephra layers that were identified in the field, with particular attention for tephra layers above and below the presumed AV-tephra layer. Analyses were performed by Thermal Ionization Mass Spectrometry at the Istituto Nazionale di Geofisica e Vulcanologia, Osservatorio Vesuviano at Napoli, using a ThermoFinnigan Triton TI multicollector mass spectrometer. The analysed samples are from the Femmina Morta (Upper and Lower tephra), Ricci, and several Borgo Hermada sites (Fig. 1).

3.2.3. Radiocarbon dating

For ^{14}C analysis of samples from immediately above and below tephra layers, plant macro remains were hand-picked under the microscope from subsamples that were obtained by sieving over a 105 or 150 μm mesh sieve to remove fines. In the selection of plant macro remains, distinction was made between plant remains from terrestrial plants and from plants growing in marshy to aquatic conditions but obtaining their carbon from the air. Remains from plants that potentially obtained their carbon dioxide from the water were excluded. In some instances, suited plant macro remains were absent and humic soil material (black organic clay with very finely divided organic matter) was used. For ^{14}C analyses, samples were subjected to the ABA pre-treatment, followed by their dating using the AMS-method, at the CIO lab in Groningen, The Netherlands. Values obtained are presented as ^{14}C years BP, and as calibrated ages BC using the OxCal4.3 software package (Bronk Ramsey, 2017) and the IntCal 13 calibration curve.

3.2.4. Particle size distribution

Particle size distributions were established by means of a Laser particle sizer (Helos KR Sympatec) at the Free University (Amsterdam). Samples were dispersed following pre-treatment with H_2O_2 and HCl to remove organic matter and calcium carbonate. Details are given as Supplemental information.

4. Results

4.1. Field observations and sampling

In the basins studied, four types of sedimentary environments were distinguished (van Gorp and Sevink, 2019): 1) oxic aquatic to marshy with peat to peaty clay; 2) anoxic marshy, with pyritic more or less peaty black clays ('pyritic clays'); 3) oxic aquatic (lacustrine/lagoonal), with calcareous gyttjas to calcareous marls ('gyttja'); 4) oxic, deltaic to fluvial, with calcareous clays to loams. The AV-layer was identified in the field as a 2–3 cm thick tephra layer with a sandy texture and a greyish-creamy colour, holding very conspicuous idiomorphic 'golden' mica and sanidine crystals, of which the mica reached sizes up to c. 4 mm. Where the tephra layer was intercalated in gyttja (such as in the interior basin of the Agro Pontino near Mezzaluna and in the coastal lagoonal deposits near Borgo Hermada, see Fig. 1), or in pyritic clays, it formed a virtually continuous horizontal layer with often sharp upper and lower boundaries, which could be followed over large distances. Intercalated in peat (marsh vegetation), it was more fragmentary and had a more variable thickness, such as at Femmina Morta (Fig. 1). However, the overall characteristics – a centimetres thick, greyish-creamy sandy tephra layer with conspicuous large mica – were invariable.

In many places the AV-layer was encountered at a depth of less than 1 m below the ground surface. In the dry summer period, the

groundwater level was generally deeper, due to deep artificial drainage starting in the thirties of the 20th century. In such cases, in peaty sediments bioturbation and mineralisation had significantly modified the original sediment characteristics, evidenced by abundant faunal excrements and biopores (mostly from earthworms), while plant macro remains were scarce. Pyritic clays had often been oxidized with the concurrent development of acid sulphate soils, marked by the presence of yellowish jarosite mottling, gypsum, and iron hydroxide mottles and concretions (Dent, 1986; Sevink, 2020). Non-affected AV-layers were encountered where the groundwater level was still high or where the layer was at greater depth (e.g. below a thick layer of fluvio-colluvial sediment and in the fills of the fluvial incisions near Borgo Hermada and in the Fondi basin).

Younger tephra was only found in the fills of fluvial incisions near Borgo Hermada in the form of a thin (c. 1 cm at maximum) fine sandy greyish layer that was intercalated in gyttja and recognized as tephra by its colour (greyish) and by the mica. It occurred a few decimetres above the AV-layer, but below any reddish-brown Early Iron Age or younger colluvial deposit (see above and Fig. 2) and was never encountered in the gyttja deposits of the central lake in the Agro Pontino, nor in the Holocene fills of the Fondi basin.

In coastal lagoonal sections in the Fondi basin, we found an older tephra layer, which occurred as a discontinuous, several centimetres thick, greyish fine sandy layer at about 20 cm below the AV-layer. Elsewhere, such as in the interior Fondi basin or in the Agro Pontino, we never encountered such older tephra layer.

General information on the sites sampled is listed in Table 1, while sampling locations are indicated in Fig. 1. In Table 1, the younger tephra layer is indicated with UT (upper tephra), while older tephra layer is indicated as LT (lower tephra).

4.2. Thin sections and mineralogy of fractions >63 μm

4.2.1. AV-layers

In the thin sections, these layers were invariably found to consist of tephra and of smaller or larger amounts of other, non-pyroclastic materials, which included clay to sand-size clastic material, well conserved plant fragments, and fossils with an amorphous silica skeleton (diatoms and sponge spicules). Additionally, some contained fossils with a calcareous skeleton and secondary carbonates (as concretions or finely divided lime). Where deposited in an anoxic environment, they furthermore held some to abundant small framboid pyrite aggregates, but generally these were oxidized to still more or less framboid iron hydroxide aggregates. The tephra largely consisted of pumice with included small phenocrysts, with in addition smaller amounts of feldspar (mostly sanidine), clinopyroxene and biotite. Other regularly encountered minerals were melanite and diopside. This mineralogical composition was rather invariable and in conformance with the composition described for proximal tephra from this eruptive phase (see e.g. Sulpizio et al., 2008; Sulpizio et al., 2010a).

The mineralogy of the fractions >63 μm was found to be very uniform, with pumice, feldspar, clinopyroxene, and mica as the main components, similar to the AV-tephra in the thin sections. Material other than tephra was hardly encountered in this fraction, apart from incidental larger sized iron concretions and rare quartz and chert grains, derived from older marine and aeolian deposits.

The AV-tephra layers thus ranged from relatively pure pyroclastic material to layers of rather mixed origin, as also described in Section 4.6. Boundaries between the tephra layer and sediments above and below were rarely abrupt at microscopic scale. Fig. 4 shows the tephra at Mezzaluna (site 405) that was deposited in a lacustrine environment with prominent accumulation of calcareous gyttja. This is reflected by the crystic plasmic fabric and abundant calcareous fossils (see Fig. 4A and B). As shown by Fig. 4C its upper boundary is abrupt, while below it is more gradual. In Fig. 5A an example is given of an AV-layer in peat (Frasso, site 500), illustrating the often rather irregular shape and discontinuous nature of this layer. Fig. 5B and C illustrate the alternation of pyroclastic material and plant fragments that characterizes the AV- layer. Additionally, in these figures the pumice fragments with their included phenocrysts and the clinopyroxenes are very well visible. Fig. 5D shows the extremely fine layering of the peat above the tephra layer as well as the irregular distribution of tephra particles, which also occur as isolated individual grains.

At Femmina Morta, the AV-tephra (site 197, sample 197-U) was deposited under rather similar conditions, i.e. in a marshy vegetation. Here, similar to the Frasso site 500, the upper and lower boundary are

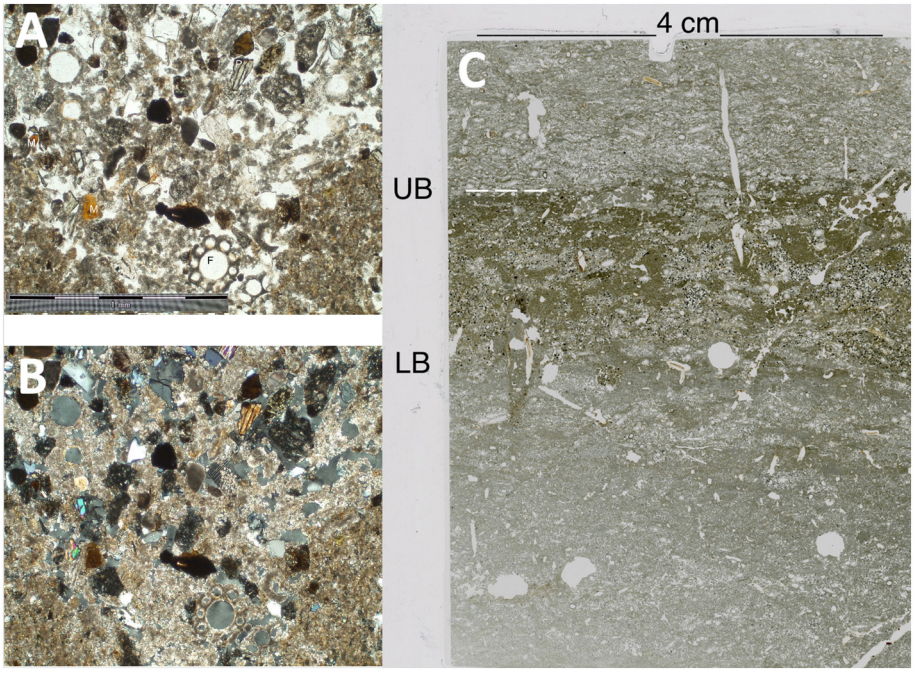

Fig. 4. AV-tephra layer at Mezzaluna (site 105). A) tephra: mostly pumice, feldspar, pyroxene (P) and some melanite (M) in a matrix of crystic plasma. F = fossil; B) as A) but with crossed nicols; C) thin section with tephra layer. LB = Lower boundary; UB = Upper boundary of tephra layer indicated with ———.

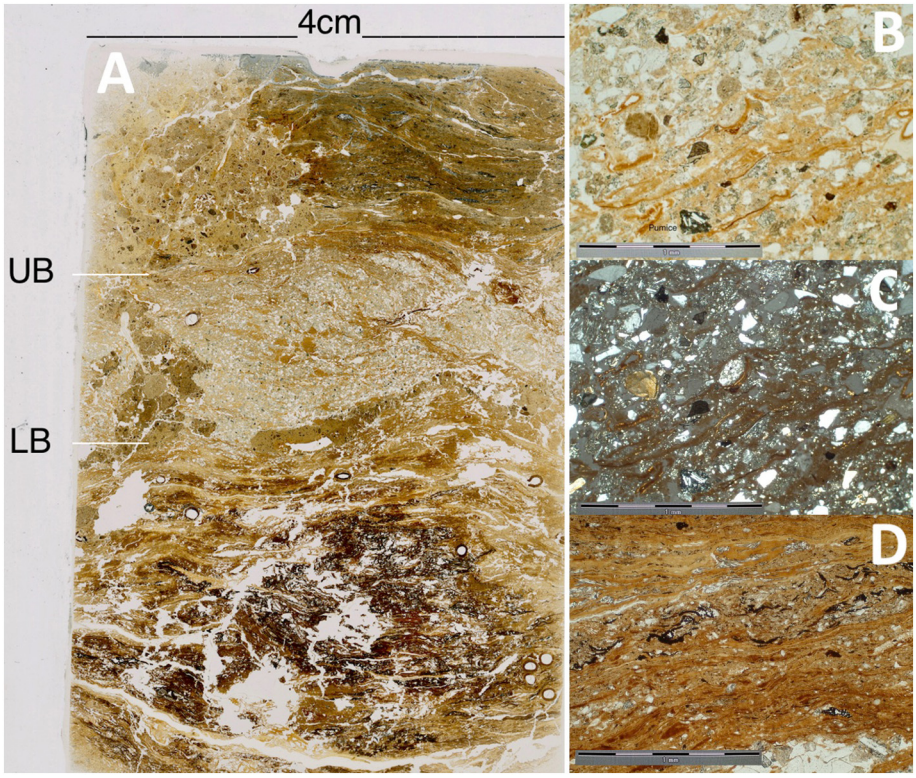

Fig. 5. AV-tephra layer in peat at Frasso (site 500): A) thin section with irregular shaped upper boundary (UB); LB = Lower boundary; B) alternation of tephra and peat; C) as B) but crossed nicols; D) finely stratified peat above the tephra layer.

relatively gradual and discontinuous (see Fig. 6A) and the tephra layer contains common diatoms and sponge spicules. Fig. 6A illustrates the dense packing of the AV-layer and a characteristic larger mica crystal (most probably phlogopite). At the Mesa site 700, where the tephra was deposited in an anoxic environment, the upper and lower boundaries are also irregular (see Fig. 7A). The oxidized pyrite shows up as black to dark brown material above the AV-layer and holds some gypsum pseudomorphs. Moreover, it contains truly abundant sponge spicules (see Fig. 7B).

4.2.2. Other tephra layers

The lower tephra layer at Femmina Morta (site 197, sample 197-L) was distinctly finer textured and less rich in pumice than the AV-layer, as evidenced by Fig. 6C and D. The figures additionally show that angular mineral fragments are common, largely consisting of feldspar (sanidine), and that the layer is discontinuous.

The upper tephra layer encountered near Borgo Hermada (sites 180 and 181) was too thin to allow for the production of a thin section in which the composition of this tephra could be reliably studied. However, study of the size fractions >63 μm showed that composition was similar to that of the AV-layer.

4.3. Chemical composition of the glasses

Samples analysed by microprobe are listed in Table 1. In a fair number of samples, glass appeared to be completely altered and fresh glass fragments were absent. In this table, they are indicated with (x). In one sample from the Fondi basin (197-L) glass shards were rare and for these only a limited number of microprobe analyses could be performed. The full set of chemical analyses can be found as Supplemental data, together with a TAS classification diagram in which all samples fall within the phonolite field, for which reason we refrain from presenting and discussing such TAS diagram.

In Figs. 8, 9, and 12, chemical data are presented in FeO vs SiO_2 and CaO vs SiO_2 diagrams, which are particularly useful for discriminating the compositionally rather similar volcanic rocks from the Neapolitan volcanoes (Sulpizio et al., 2010c; Zanchetta et al., 2011). The data are presented together with the chemical composition of glass from tephra erupted from the Neapolitan volcanoes between ca. 2.5 (distinctly before the AV-eruption) and 1.0 ka BC (before the deposition of the colluvio-alluvial deposits, linked to early agriculture, e.g. Attema, 2017). Literature data for the relevant eruptions that occurred in the time span mentioned have been plotted as coloured fields for comparison with our data (Fig. 8). They include products of the following eruptions: AV and AP (between AV and Pompei; Di Vito et al., 2013) from Somma-Vesuvius (Andronico and Cioni, 2002; Santacroce et al., 2008; Sulpizio et al., 2008, 2010c), and Agnano-Monte Spina, Astroni and Capo Miseno from Campi Flegrei (Tonarini et al., 2009 and references therein; Arienzo et al., 2010 and references therein, Smith et al., 2011; Jouannic et al., 2013; Arienzo et al., 2016; Margaritelli et al., 2016).

Fig. 8 highlights that our samples form three clusters. Samples 197-U, 122 and 198-L, from the Femmina Morta, Fondi inland, and Borgo Hermada locations, plot in the field built on Avellino literature data. Sample 181-U from Borgo Hermada is marked by high FeO contents with respect to all other analysed samples and resembles the first AP eruptions. Glasses from the lowest tephra layers from Tumulillo and Femmina Morta (1005-L and 197-L) plot in the field of the Agnano-Monte Spina and Astroni glasses.

4.3.1. Fondi basin

At Femmina Morta (site 197) an upper and a lower tephra layer were found of which the upper exhibited the field characteristics of the AV-layer (see Section 4.1). This upper tephra (sample 197-U) is phonolitic in composition and in terms of major elements is similar to the Avellino glasses, as highlighted by the Total Alkali vs. Silica data (not shown) and by the FeO vs SiO_2 diagram (Fig. 8). In Fig. 9A, our

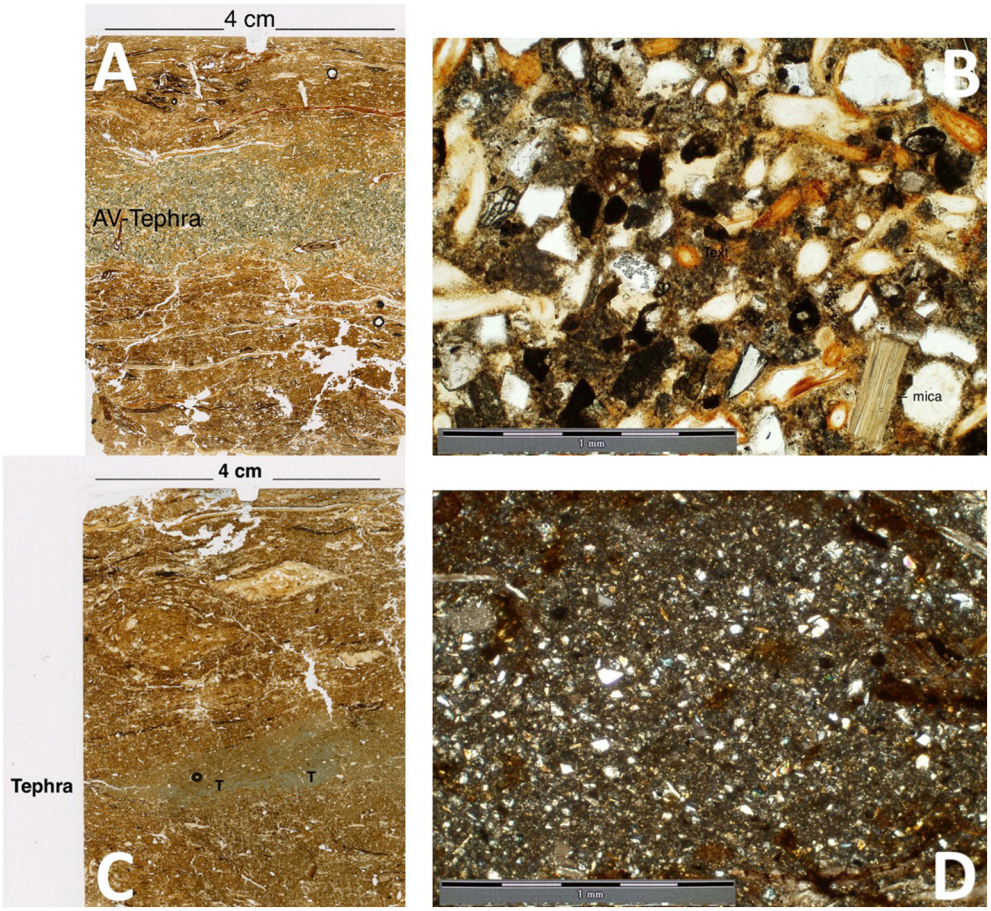

Fig. 6. Tephra layers in peat at Femmina Morta (site 197): A) thin section AV-layer (197-U); B) detail of AV-layer with mica crystal.; C) thin section Astroni 6-layer (197-L); D) detail of Astroni 6-layer with abundant angular feldspar.

samples fall in the AV EU3-EU5 fields. They have a CaO content of around 2 wt%, while SiO_2 varies from 51 to 58 wt%. Samples 197-U-1, -2 and -3 are from the upper, middle and lower part of the AV-layer and were analysed to assess whether temporal variation exists in the composition of this layer. The results point to absence of such variation. For the lower tephra layer (sample 197-L) only two analyses could be performed on glass shards and these are trachytic in composition. The high silica content (Fig. 9B) is likely due to the relatively low sum of major oxides (less than 94%), which in the calculation of the total element contents on anhydrous basis significantly increases the content of the most abundant element (SiO_2). Henceforth, the upper layer (197-U) can be attributed to the Avellino eruption, whereas the lower layer (197-L) falls in the proximity of the Astroni/Agnano-Monte Spina field.

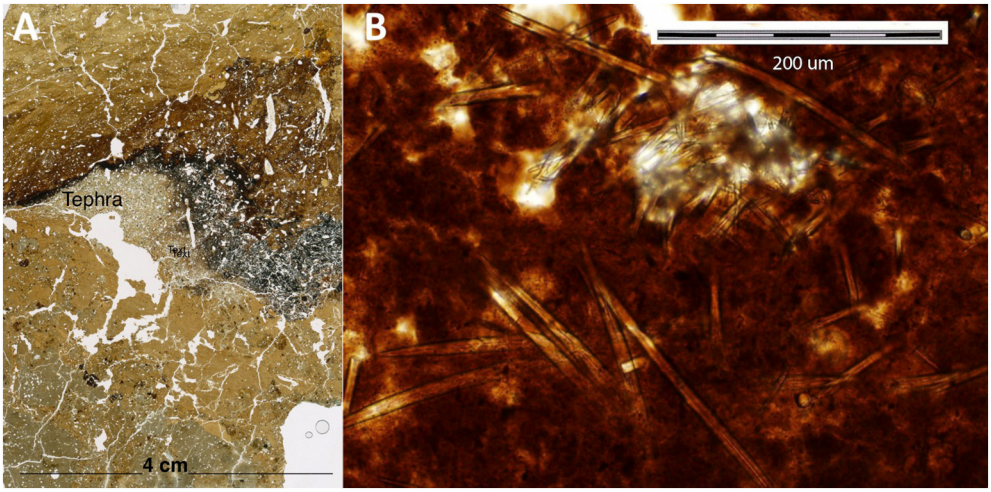

Fig. 7. AV-tephra layer in peat at Mesa (site 700): A) thin section; B) detail of pyritic sediment above the AV-layer with abundant sponge spicules.

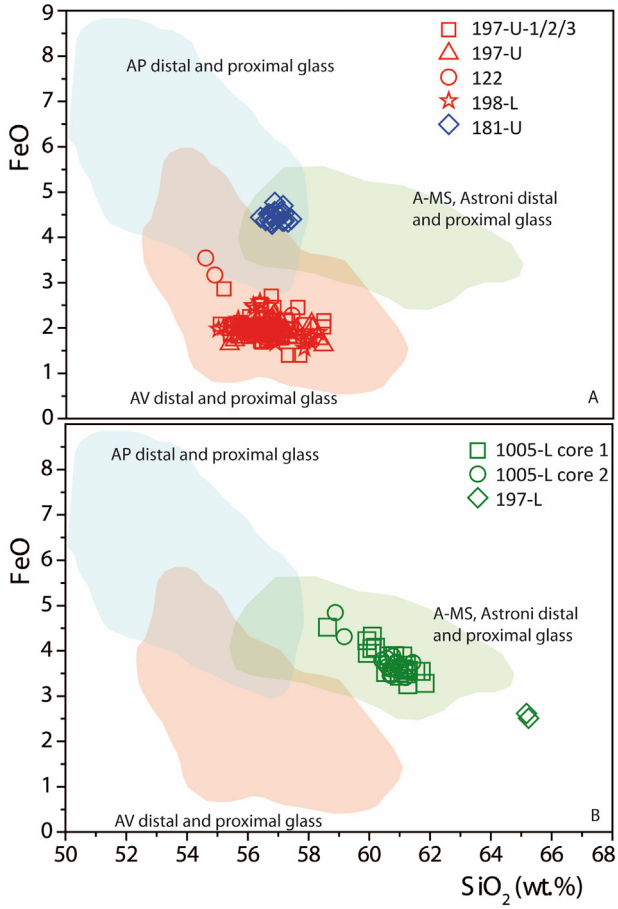

Fig. 8. Diagrams showing FeO versus SiO_2 percentages for glass shards from various tephra layers and relevant compositional fields. 197-U-1/2/3/ = samples of top/centre/bottom of the AV-layer; 197-U = second sample from the AV-layer; 1005-L core 1 = sample from first core; 1005-L core 2 = sample from second core.

At Tumolillo (site 1005), in the coastal area towards Sperlonga, two cores were studied, both with two tephra layers of which the upper was identified as the AV-layer based on its field characteristics. Glass shards from this tephra layer have been sampled, but due to the absence of unaltered glass shards it was impossible to analyse the chemical composition by electron microprobe. Results for glass shards from the lower tephra in core 1 (1005-L-1) and core 2 (1005-L-2) indicate that they are trachy-phonolitic. In Fig. 9B they overlap the Astroni 3, 6, Capo Miseno, and Agnano Monte Spina glass compositions. CaO varies from about 3.5 to 2 wt%, and SiO_2 from about 58 to 62 wt%.

At Fondi inland (site 122) the tephra layer observed was identified as the AV-layer based on its field characteristics. In terms of chemical composition, glass shards from this layer are phonolitic and similar to samples 197-U and 197-U-1/2/3 (Figs. 8, 9A). In other words, their composition is similar to that of glass from the AV-eruption.

4.3.2. Agro Pontino basin

Attempts to analyse glass shards from tephra layers at Ricci (site 216) and Mesa (site 700), both identified as AV-layer on the basis of their field characteristics, failed because the samples studied did not contain fresh glass shards. For the Borgo Hermada area (see Fig. 1) tephra layers from two cores (sites 181 and 198) were studied, while in the core at site 180 glass was found to be absent in the tephra layer. In core 181 two tephra layers were encountered, of which the lower was identified as the AV-layer based on its field characteristics. Glass shards from the upper tephra layer have been analysed (sample 181-U). In the TAS diagram (not shown; see Supplementary data) they plot in the phonolite field close to the tephrite-phonolite/phonolite boundary. The stratigraphic position (above the AV-tephra layer), the Na_2O/K_2O vs SiO_2 (not shown; see Supplementary data), the FeO vs SiO_2, and the CaO vs SiO_2 diagrams (Figs. 8 and 9C) allow for its attribution to the post-AV events of the Somma-Vesuvius. This is confirmed by the results for site 198, in which the lower tephra (sample 198-L) is an alkali-rich phonolite compositionally similar to samples 197-U, 197-U-1/2/3, 122, and its glasses plot within the compositional field of the AV-tephra.

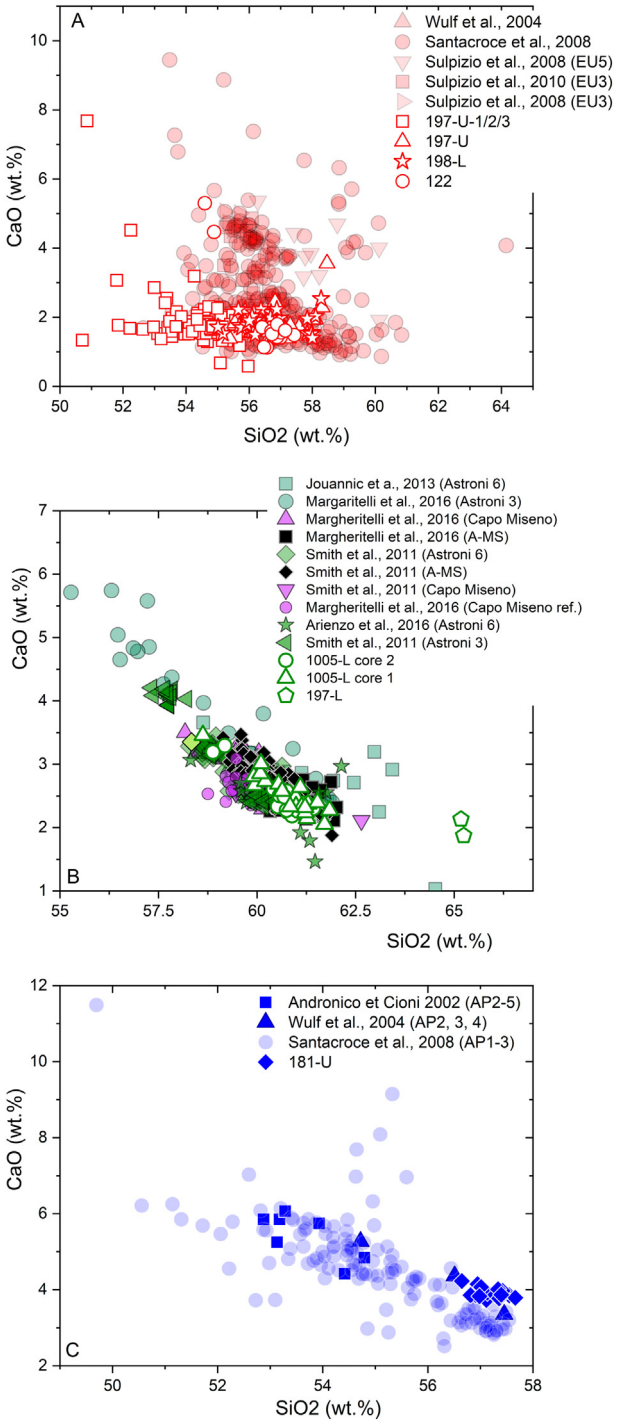

Fig. 9. CaO versus SiO_2 diagrams for: A) Samples 197-U and 197-U-1/2/3, 198-L, 122 plotted together with literature data for glasses of AV eruption products; B) Samples 1005-L core 2, 1005 – L core 1, 197-L plotted together with literature data for glasses of Astroni, Capo Miseno and Agnano-Monte Spina eruption products; C) Sample 181-U plotted together with literature data for glasses of products of the AP eruptions.

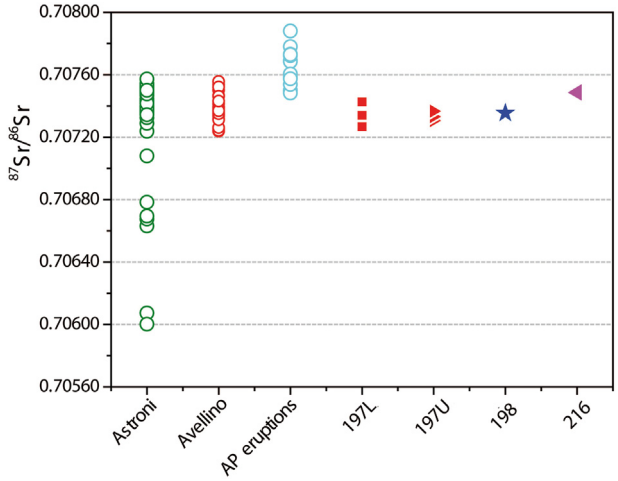

Fig. 10. Strontium isotopic ratios for some samples from the Agro Pontino and Fondi basin, and literature-based ratios for relevant tephra eruptions.

4.4. Isotope composition

In Fig. 10 results for the samples analysed are graphically presented, while analytical results are also presented as Supplementary data. The Sr isotope composition of feldspars from the Femmina Morta upper and lower tephra (197-U and 197-L) are similar (c. 0.7073) and are in the range of data obtained for minerals and glass from both the Avellino and Astroni erupted products (Civetta et al., 1991; Tonarini et al., 2009; Arienzo et al., 2015; unpublished data by Arienzo). Another aliquot of feldspars and the clinopyroxenes from sample 197-L have $^{87}Sr/^{86}Sr$ ratios of c. 0.7074 and 0.7073, respectively. Feldspars from the Ricci site 216, where the occurrence of AV-tephra was hypothesized based on field characteristics of the intercalated tephra layer, have slightly higher $^{87}Sr/^{86}Sr$ ratios (0.7075) than the feldspars from 197-L. These isotope compositions are still within the range for Avellino products.

Comparing our results with those on the various relevant eruptions taken from the literature, it is evident that Sr-isotopic compositions do not allow for discrimination between the Somma-Vesuvius and Campi Flegrei eruptions that occurred within the studied time span. However, they clearly demonstrate that an Ischia origin of these tephra can be ruled out since isotope compositions of the Ischia volcanics (bulk rocks, glasses and minerals) are in the range of 0.7050 to 0.7069 (e.g. Petrini et al., 2001; D'Antonio et al., 2007, 2013; Iovine et al., 2017a, 2017b, 2018 and references therein), i.e. they are less enriched in radiogenic Sr relative to volcanic material from the Campi Flegrei and Somma-Vesuvius.

4.5. ^{14}C dating

In Table 2 results are presented for all sites studied. Earlier datings on relevant sites - Migliara 44.5 (44.5), Campo Inferiore (Campo), Ricci (Ricci), Mezzaluna (405), and Tratturo Caniò (455) - are in italics. In this table, the data on the nature of the samples evidences the sometimes very low content of suited plant macro remains, both in earlier sections (44.5) and in new sections (700). For these sites, humic clay had to be used for dating given the absence of such suited remains. Some sections near Borgo Hermana (362, 601, 602) did not contain any suited plant macro remains or humic clay above or below that AV-layer and therefore could not be analysed.

The upper (post-AV) tephra layers at Borgo Hermada (sites 180 and 181) were in unsuited sediment (gyttja) and did not contain reliable plant macro remains. By contrast, for the lower tephra layer occurring at Femmina Morta (sample 197-L) and Tumolillo (1005-L) suited plant macro remains were found. The ages obtained for Femmina Morta (197-L) are quite remarkable, being virtually identical for all samples dated (1, 2, 3, and 5), for which reason sampling was repeated and new datings were performed on *Cladium mariscus* seeds. The new ages obtained are strikingly similar to the earlier datings, performed on other macro plant materials. At Tumolillo, datings for the lower tephra layer are 3720 ± 25 BP (below) and 3765 ± 25 BP (above) (Table 2), constraining the age of this layer to 2201–2053 cal BC (95.4% probability).

Table 3 provides an overview of the AV-layer related samples. Samples from below this layer are similar in radiocarbon age, with the exception of Femmina Morta (site 197). Excluding the latter dating, the mean age is c. 3570 BP. Ages obtained for samples from above exhibit a far wider age range: For the sites 44.5 and Campo ages are distinctly higher than the mean age obtained for the samples from below the AV-layer, whereas the ages for Mesa site 700 and Borgo Hermada site 362 are distinctly younger (3085 and 3415 BP).

4.6. Grain size analyses

Fig. 11 shows the location of the sites where tephra was sampled and the median grain sizes for the various samples. Median values for 44.5 and Campo are from Sevink et al. (2011). The values exhibit a gradual fining with increasing distance to the Somma-Vesuvius. In Fig. 11, in addition, grain size distributions are presented for a series of tephra samples, demonstrating this gradual shift in median values. These graphs include samples from nearly pure tephra (405 and 334) and from tephra in clayey sediment (399 and 508). The earlier tephra from Femmina Morta (197-L) is distinctly less sorted and finer textured. A full set of grain size analyses is presented as Supplemental data.

5. Discussion

5.1. Identification of the tephra layers

Field characteristics of all tephra layers studied and indicated as 'AV' in Table 1 were a centimetres thick greyish-creamy sandy tephra layer with conspicuous mica and abundant mineral fragments. Whenever more than one tephra layer is encountered, evidently the well-established Mid to Late Holocene tephrochronostratigraphy for Central Italy can be used (see e.g. Santacroce et al., 2008; Giaccio et al., 2009; Zanchetta et al., 2011; Jouannic et al., 2013; Jung, 2017). Relevant are those eruptions that date between c. 2500 and c. 1000 BCE. The lower limit is based on the available ^{14}C datings, the second, upper time limit on the dating of the onset of massive deposition of colluvio-alluvial sediments in the Agro Pontino and Fondi basin (see Van Joolen, 2003; Feiken, 2014; Attema, 2017). Given these time constraints, relevant eruptions for our area of study are the larger Campanian ones, for which chemical data are presented in the Figs. 8 and 9. Other more remote major volcanoes have been active in this period, such as the Ischia and Etna volcanoes, but the chemical and isotopic composition of their tephra differs from that of the tephra we found. Moreover, tephra from these other volcanoes and dating from the studied time span has never been reported for Southern Lazio (see e.g. Jouannic et al., 2013; Margaritelli et al., 2016).

The chemical composition of volcanic glasses from the various relevant Campanian eruptions is well known and can be readily used, in case that field macro characteristics and stratigraphy are insufficient to distinguish between tephra from the Somma-Vesuvius and Campi Flegrei. Results for the samples studied are presented in Fig. 8, together with literature data (Wulf et al., 2004; Santacroce et al., 2008; Sulpizio et al., 2008, 2010c; Tonarini et al., 2009; Arienzo et al., 2010, 2016; Smith et al., 2011; Jouannic et al., 2013; Margaritelli et al., 2016). The data demonstrate that glasses from the AV-tephra that we analysed have a very similar chemical composition, which is in line with the homogeneous mineralogical composition of the tephra layers that we observed, both in the field and in thin section. AV glasses are characterized

Table 2
Overview of radiocarbon datings for the sites from the Agro Pontino and Fondi basin. Earlier published datings are in italics.

Locations	Site	Description of sample	Material	Sample number CIO	Age BP	Delta 13C	Calibrated age	References
Agro Pontino								
Migliara 44.5	44.5	Top layer 4, above AV-tephra layer	Black humic clay/peat	GrA-46206, 46208	*3635 +/− 25*	*−27.75*	*2126–1923 cal BC*	Sevink et al., 2011
		Base layer 4, above tephra layer	Black humic clay/peat	GrA-46203, 46205	*3685 +/− 25*	*−27.10*	*2189–1978 cal BC*	
		Top layer 2, below AV-tephra layer	Black humic clay/peat	GrA-46200, 46201	*3565 +/− 25*	*−27.79*	*2014–1781 cal BC*	
Campo inferiore	Campo	Above AV-tephra layer	Wood fragment from peat	GrA-46210	*3610 +/− 30*	*−28.98*	*2110–1889 cal BC*	Sevink et al., 2011
		Above tephra layer	Wood fragment from peat	GrN-32454	*3635 +/− 40*	*−27.58*	*2135–1896 cal BC*	
		Below AV-tephra layer	Tree leaves	GrA-45134, 45265, 45266	*3585+/− 20*	*−29.49*	*2016–1886 cal BC*	
		Below tephra layer	Wood: thick branch	GrA-45003, 45006, 45256, 45257	*3565 +/− 20*	*−24.94*	*2009–1826 cal BC*	
		Below tephra layer	Tree trunk: outer 2–5 rings	GrA-45042, 45032, 45254, 45255	*3715 +/− 15*	*−27.49*	*2195–2036 cal BC*	
		Below tephra layer	Tree trunk: core	GrA-45007, 45008, 45259, 45260	*3690 +/− 15*	*−27.07*	*2136–2031 cal BC*	
Ricci	Ricci	Wood in EBA II or MBA I vessel	Wood	GrA-51750	*3445 +/− 35*	*−26.94*	*1881–1665 cal BC*	Bakels et al., 2015
		At 218 cm (AV-tephra layer: 211 cm)	*Alnus* seed and catkin	GrA-56630	*3600 +/− 45*	*No result*	*2131–1780 cal BC*	
		Below AV-tephra layer: burnt patch of peat	Charcoal terrestrial plants	GrA-56678	*3640 +/− 35*	*−28.12*	*2135–1912 cal BC*	
		At 248 cm (AV-tephra layer: 211 cm)	*Schoenoplectus* seeds	GrA-56801	*3885 +/− 35*	*−25.99*	*2471–2214 cal BC*	
Tratturo Caniò	455	Layer 5001 (above AV-tephra layer)	Charcoal terrestrial plants	GrA-44910	*3495 +/− 45*	*−25.56*	*1936–1693 cal BC*	Feiken et al., 2012
Mezzaluna	405	Tree trunk from immediately below gyttja	Wood	GrA-51749	*3565 +/− 35*	*−27.16*	*2023–1776 cal BC*	Bakels et al., 2015
		Tree trunk from immediately below gyttja	Wood: *Alnus* (outer tree rings)	GrM-17418	3735 +/− 25	−26.36	2205–2036 cal BC	
Frasso	500	Above AV-tephra layer (within 2 cm)	Wood (twig)	GrM-17223	3505 +/− 25	−25.66	1897–1749 cal BC	
		Above AV-tephra layer (within 2 cm)	Charred seeds terrestrial plants	GrM-17840	3365 +/− 40	−21.36	1749–1532 cal BC	
		Below AV-tephra layer (within 2 cm)	Wood (twig)	GrM-17225	3530 +/− 25	−25.09	1935–1771 cal BC	
		Below AV-tephra layer (within 2 cm)	Charred seeds terrestrial plants	GrM-17226	3610 +/− 25	−26.83	2031–1897 cal BC	
Mesa	700	Black peat/clay, 0–1 cm above AV-tephra layer	Black humic clay	GrM-17888	3085 +/− 35	−27.69	1749–1532 cal BC	
		Black peat/clay, 0–3 cm below AV-tephra layer	Black humic clay	GrM-17495	3590 +/− 25	−27.60	2022–1887 cal BC	
Borgo Hermada	362	BE 362 57–58 cm, tephra (AV) at 60–62 cm	*Schoenoplectus lacustris* seeds	GrM-17231	3415 +/− 25	−23.60	1861–1639 cal BC	
	601	601–1 70–73 cm: AV-tephra at 60–61 cm	Twig/leaf	GrM-17890	210 +/− 40	−29.40	unreliable	
	602	602–1121–127 cm: AV-tephra at 112–115 cm	*Schoenoplectus lacustris* seeds	GrM-17907	3570 +/− 25	−27.76	2017–1784 cal BC	
Fondi								
Femmina Morta	197	FM 7 42–50 cm: Above AV-tephra layer (52–54 cm)	*Corylus*/*Viburnum* wood	GrA-67046	3380 +/− 35	−27.88	1762–1562 cal BC	Doorenbosch and Field, 2019
		FM 5 54–56 cm: Below AV-tephra layer (52–54 cm)	Leaf fragment of terrestrial plant	GrM-16626	3495 +/− 25	−26.01	1891–1746 cal BC	
		FM 5 54–56 cm: Below AV-tephra layer (52–54 cm)	*Cladium mariscus* seeds	GrM-18970	3488 +/− 25	−25.59	1887–1744 calBC	
		FM 3 64–66 cm: Above Astr-tephra layer (66–68 cm)	Wood and *Cladium mariscus* seeds	GrM-16625	3510 +/− 25	−25.68	1906–1751 cal BC	
		FM 3 64–66 cm: Above Astr-tephra layer (66–68 cm)	*Cladium mariscus* seeds	GrM-18971	3528 +/− 25	−23.94	1932–1770 cal BC	
		FM 2 68–70 cm: Below Astr-tephra layer (66–68 cm)	*Cladium mariscus* seeds	GrM-16624	3525 +/− 35	−27.12	1943–1751 cal BC	
		FM 2 68–70 cm: Below Astr-tephra layer (66–68 cm)	*Cladium mariscus* seeds	GrM-18972	3532 +/− 25	−23.73	1939–1771 cal BC	
		FM 1 70–78 cm: Below Astr-tephra layer (66–68 cm)	*Quercus* twig	GrA-68587	3535 +/− 35	−30.67	1956–1751 cal BC	
Tumolillo	1005	90–91 cm: Below AV-tephra (88–90 cm)	*Cladium mariscus* seeds	GrM-16620	3550 +/− 30	−24.71	2009–1772 cal BC	
		90–91 cm: Below AV-tephra (88–90 cm)	Charcoal terrestrial plants	GrM-17417	3570 +/− 25	−25.15	2017–1784 cal BC	
		111–112 cm: Above Astr-tephra (112–114 cm)	*Lycopus europaus*, *Cladium mariscus* seeds	GrM-16621	3765 +/− 25	−26.97	2286–2057 cal BC	
		114–115 cm: Below Astr-tephra (112–114 cm)	*Lycopus europaus*, *Cladium mariscus* seeds	GrM-16622	3720 +/− 25	−26.66	2199–2035 cal BC	
Fondi inland	122	122A 79–80 cm: Above AV-tephra (81–83 cm)	Large *Schoenoplectus lacustris* seed	GrM-17887	3500 +/− 50	−29.40	1947–1691 cal BC	
		122A 83–84 cm: Below AV-tephra (81–83 cm)	Charcoal terrestrial plants	GrM 17227	3555 +/− 25	−26.58	2007–1776 cal BC	
		122A 85–86 cm: Below AV-tephra (81–83 cm)	Charcoal terrestrial plants	GrM 17228	3580 +/− 25	−25.79	2022–1882 cal BC	

Table 3
Radiocarbon datings (non-calibrated ages) for samples from below and above the AV-layer.

Locations	Name/number	Below tephra layer	Age BP	s.d.	Material
Agro Pontino					
Migliara 44.5	44.5	Top layer 2, below tephra layer	3565	25	Org. matter
Campo inferiore	Campo	Below tephra layer	3585	20	Tree leaves
Mezzaluna	405	Tree trunk from immediately below gyttja	3565	35	Bark tree trunk
		Below tephra layer (within 2 cm)	3530	25	Wood
Frasso	500	Below tephra layer (within 2 cm)	3610	25	Charred seeds
Mesa	700	Black peat/clay, 0–3 cm below tephra layer (C2)	3590	25	Org. matter
Fondi					
		FM 5 54–56 cm: below tephra layer (52–54 cm)	3495	25	Leaf fragment
Femmina Morta	197	FM 5 54–56 cm: below tephra layer (52–54 cm)	3488	25	Seeds
		Tumolillo 90–91 cm: below tephra (88–90 cm)	3550	30	Seeds
Tumolillo	1005	Tumolillo 90–91 cm: below tephra (88–90 cm)	3570	25	Charcoal
		Fondi 122A 83–84 cm: below tephra (81–83 cm)	3555	25	Charcoal
Fondi 122	122	Fondi 122A 85–86 cm: below tephra (81–83 cm)	3580	25	Charcoal

Locations	Name/number	Above tephra layer	Age BP	s.d.	Material
Agro Pontino					
Migliara 44.5	44.5	Base layer 4, above tephra layer	3685	25	Org. matter
Campo inferiore	Campo	Above tephra layer	3635	40	Wood
Ricci	Ricci	Wood in EBA II or MBA I vessel	3445	35	Wood
Tratturo Caniò	455	Layer 5001 (above tephra layer)	3495	45	Charcoal
Frasso	500	Above tephra layer (within 2 cm)	3505	25	Wood
Mesa	700	Black peat/clay, 0–1 cm above tephra layer	3085	35	Org. matter
Borgo Hermada 362	362	BE 362 57–58 cm, tephra (AV) at 60–62 cm	3415	25	Seeds
Fondi					
Femmina Morta	197	FM 7 42–50 cm: above tephra layer (52–54 cm)	3380	35	Wood
Fondi inland	122	Fondi 122A 79–80 cm: above tephra (81–83 cm)	3500	50	Charcoal

by low FeO content relative to the AP glasses. The largest differences are with the later AP eruptions (AP3–6), but these tephra are not relevant for our study, since the AP3–6 eruptions are distinctly younger than the upper time limit of 1000 BCE (see e.g. Santacroce et al., 2008).

In most cases, we could readily obtain additional evidence (other than field macro characteristics and stratigraphy) for the nature of the tephra layers (AV, Lower or Upper Tephra with respect to AV) encountered in the various sections, such as their radiocarbon age. Sites for which ^{14}C dating was impossible include Borgo Hermada site 601 and the sites listed under 'Other' in Table 1. Among the latter are the Borgo Hermada sites 180 and 181, at which the post-AV tephra layer encountered (samples 180-U and 181-U) could not be radiocarbon dated (for

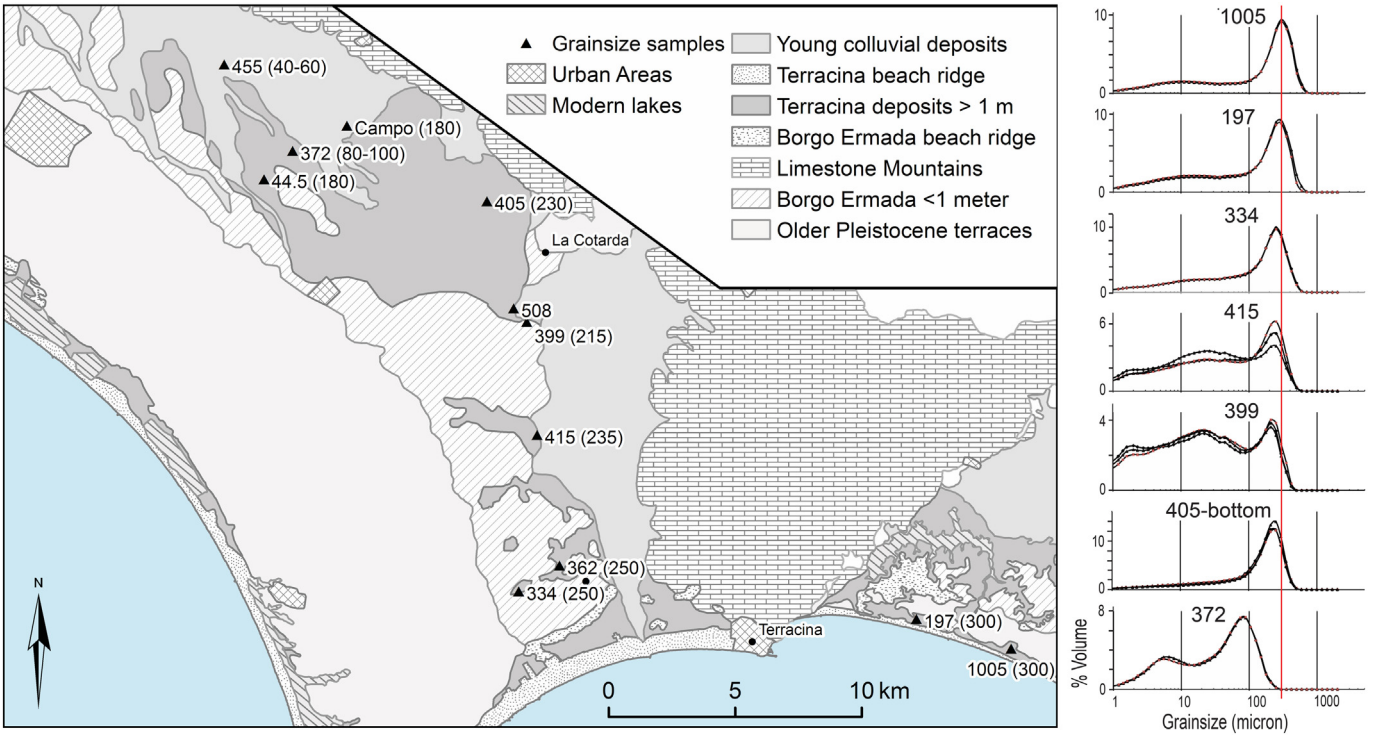

Fig. 11. Location of sites for which grain size of the AV-layer has been established and their median grain size (between brackets). Right: Histograms illustrating the fining trend with increasing distance.

arguments, see Section 4.5). In case of site 181, the attribution of the upper tephra layer to a post-AV eruption is corroborated by the chemical composition of the lower tephra, which confirms its attribution to the AV-eruption (see Figs. 8 and 9). As to the upper tephra layer in the section at site 181 (181-U), this can be ascribed to the AP1–2 eruption on the basis of its glass chemistry (see Figs. 8 and 9).

The upper tephra layer must have been deposited relatively shortly after the AV-event (see also van Gorp et al., 2020) and represents a significant eruptive event, implying that this layer has to be attributed to the AP2 eruption, the AP1 eruption being of minor magnitude (see Santacroce et al., 2008). Magny et al. (2007) identified a tephra layer at the Lago di Accesa (Tuscany), which they ascribed to the inter-Plinian AP2-AP4 events ('or ending phase of Avellino event'), clearly postdating the Avellino event with a few centuries, based on its chemistry and ^{14}C datings. Tephra at Lago di Accesa, originating from the Vesuvius, evidently must have passed over the Agro Pontino and our identification of the post-AV tephra layer as probably linked to the AP2 eruption is in line with their results.

As to the tephra layer encountered in the Fondi basin below the AV-layer (sample 197-L), the chemical data evidence that this tephra is of Phlegraean origin (see Figs. 8 and 9B). The major potentially relevant eruption of the Campi Flegrei is the Agnano-Monte Spina eruption, of which the tephra is widely distributed over the Central Mediterranean, but this eruption is considerably older (4690–4300 cal ka BP, see e.g. Iovine et al., 2017a, 2017b; Blockley et al., 2008) than the analysed tephra (see Table 2: c. 4 ka BP). For Tumolillo (site 1005), the chemical data combined with the ^{14}C datings and Central Italian tephrostratigraphy leads to the attribution of the tephra found below the AV-layer to the latest major Phlegraean eruption, the Astroni 6 eruption (Tonarini et al., 2009 and references therein; Smith et al., 2011). At first sight, the ^{14}C datings from the Femmina Morta sequence (site 197) would not support the attribution of its lower tephra layer to the Astroni eruptions, but these datings are not reliable, as will be discussed in more detail in Section 5.3.

The occurrence of tephra from the Astroni eruption is in line with the results from Jouannic et al. (2013), who reported tephra from the Astroni eruption to occur in the Maccarese core and found similar ^{14}C ages for this layer. Astroni tephra was also found in the Gulf of Gaeta core by Margaritelli et al. (2016) and Di Rita et al. (2018), but it was ascribed to the Astroni 3 eruption that is slightly older (4098–4297 cal BP: Smith et al., 2011). Margaritelli et al. (2016) recognize a slightly younger tephra, which they attribute to Astroni 6 or Capo Miseno. The Astroni 6 eruption has been dated at between 4098–4297 cal BP and 3978–4192 cal BP (Smith et al., 2011), whereas the Capo Miseno eruption has been $^{40}Ar/^{39}Ar$ dated at 3700 ± 500 y BP (Di Renzo et al., 2011) and 5090 ± 140 y BP (Insinga et al., 2006). The chemical composition of Astroni 6 glass is shown in Fig. 12A, together with the composition of glasses attributed by Margaritelli et al. (2016) to Campo Miseno. All glass samples display the same variability in terms of CaO and SiO_2 contents and this variability is higher than that of Capo Miseno glasses (purple circle in Fig. 12B).

The overlap among the dates and chemistry seriously hampers a univocal attribution based on the chemical data. However, volcanological features of these two eruptions strongly support an attribution of the lower tephra to the Astroni 6 event. The Astroni 6 event, with the widest distributed tephra of the various Astroni events (Isaia et al., 2004) and following on the Astroni 3 event, was a sub-Plinian eruption, and its tephra was distributed over a large part of the Campanian Plain, whereas Capo Miseno produced a tuff cone, without evidence for the generation of high eruption columns and with deposits distributed in only a limited area around the vent.

5.2. Radiocarbon ages and their implications

^{14}C dating is fundamental in tephrostratigraphy and can be decisive in case that chemical data are not available (absence of suited glass

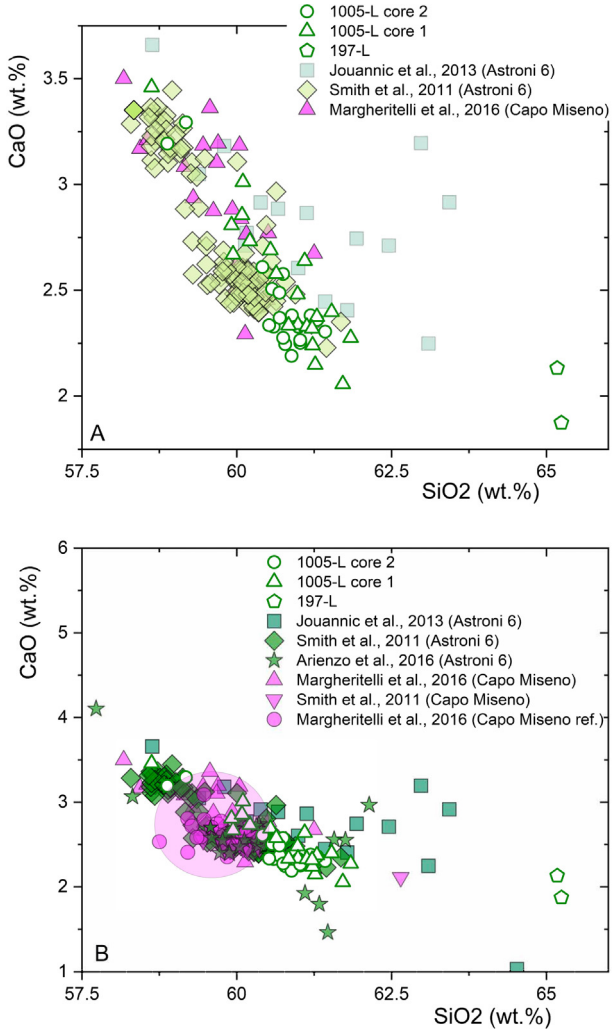

Fig. 12. A) CaO versus SiO_2 diagram displaying the chemical variability of Astroni 6 (new and literature data) and Capo Miseno glasses (literature data). Glasses from the Astroni 6 eruption are characterized by a larger chemical variability relative to the Capo Miseno glasses. In fig. B the latter are included in the purple circle. (For interpretation of the references to colour in this figure legend, the reader is referred to the web version of this article.)

fragments in the tephra layer analysed, or not analysed) or other criteria (see Section 5.1) are not applicable. ^{14}C analyses allow to constrain the age of a tephra deposit and thus its identification, but not all sections studied contained suited plant macro remains.

Marked differences exist in the range of ages obtained for materials from below the AV-layer and for those from above (Table 3). Samples from below the AV-layer exhibit a very small range in age, i.e. 3530–3585 years BP, with a mean value of 3570 ± ca. 25 years BP, setting a clear lower age limit for the AV-layer, which is in line with the age of c. 1900 cal BC obtained by Alessandri (2019). These datings alone already allow for identification of the related tephra layer as the AV-layer. The only deviating value is that for Femmina Morta (site 197, see later).

As to the ages obtained for materials directly above the AV-layer, a first conclusion that can be drawn based on the above discussed results is that the ages published earlier by Sevink et al. (2011) for samples from Migliara 44.5 and Campo Inferiore (3685 and 3635 years BP, respectively) are to be considered as too old, a conclusion that was also drawn by Alessandri (2019). Even when excluding these ages, variations in age remain considerable (from 3505 to 3085 years BP). This evidently asks for an explanation, which might be sought in the low sedimentation rate after tephra deposition and eventually a post-

tephra hiatus. The aberrant ages found for the Femmina Morta samples (site 197) cannot be attributed to such hiatus or low sedimentation rate. Being systematically too young and also of similar age, we attribute these to post-Avellino 'homogenisation' by bioturbation. Evidence for such bioturbation was observed in the thin sections (see biopores above AV-tephra in Fig. 6A).

Biases in the ^{14}C dating of samples from above the presumed AV-layers do not prevent a reliable identification of these layers as AV-tephra, which can also be based on the results of other analytical methods used (see Table 1) or, in some cases, on the radiocarbon age of samples from immediately below. These biases and their implications for attempts to radiocarbon date the tephra layers from the coastal basins of southern Lazio will be discussed in a separate paper (Sevink et al., 2020, submitted).

5.3. Spatial variation in sedimentological and lithological features of the AV-layer

Microscopic study of fractions >63 μm from all AV-layer samples on which analyses have been performed (see Table 1) and of the thin sections showed that compositional variation in the tephra is limited to slight differences in the ratio pumice/mineral fragments – somewhat fewer pumice in tephra layers from the peat and pyritic clay samples relative to the gyttja samples. This is corroborated by the limited variation in the chemical composition of the glass analysed, both in space and time (see the Supplementary data on AV samples 122, 198 and 197-U, including subsamples 1, 2 and 3, and Figs. 8, 9) and is not unexpected, since it is not likely for significant temporal variation in composition of the distal tephra to occur during such single phase of a large eruptive event. Nevertheless, it is clear that some fining occurred with increasing distance from the vent. This fining is in line with the observations by Sulpizio et al. (2010b), but the sorting they observed, both with regard to grain size and components, concerns sorting close to the eruption centre (at maximum c. 30 km and within the EU5 isopach of 5 cm), rather than the truly distal fining observed by us for a distance range of 100–145 km. Lastly, within the tephra layer itself, no indications were found for temporal variation in grain size of the tephra, peak values being rather identical (see Supplemental data, samples 334 and 405 in Fig. 11).

The fining trend is distinct, but the data need to be interpreted with care, as evidenced by the marked differences in grain size between the tephra studied by Sevink et al. (2011) and the recent analyses for nearby tephra sites (see Fig. 11 and Supplemental file 2, sample 372 and 455). The earlier data were based on sieving after sample pre-treatment and removal of the fraction <50 μm (by sieving), instead of a full analysis using the Laser scan technique (see Materials and methods). Moreover, a number of samples exhibited a bimodal or even more complex composition, such as samples 508 and 372.

A typical example of a deviating composition comes from the deltaic to fluvial complex at Tratturo Caniò. Its sample (455) exhibits two major peaks at c. 6 and 20–50 μm, and a third far less conspicuous peak at slightly over 200 μm. It is most probably only this third peak that can be linked to the tephra. This would fit very well the data for the most nearby sites Migliara 44.5 (sample 44.5) and Campo inferiore (sample Campo), and strongly suggests that the coarser silt fraction is largely of biotic origin. The sedimentary facies at Tratturo Caniò is a fluvial to deltaic levee, transitional to a basin, explaining the overall silty character of the sediment. Samples from La Cotarda, site 508 exhibit a similar pattern, with a third slight peak at c. 250 μm, whereas those from Ricci, site 372 suggest an even more complex origin and significant reworking of the original tephra, which given the facies (fluvio-deltaic) is quite likely.

In summary, samples from relatively tranquil (non-fluvial) sedimentary environments clearly exhibit a decreasing size of the dominant tephra fraction with increasing distance from its source and its non-calcareous fraction consists of tephra with varying amounts of siliceous skeletal remains, whereas in more fluvial to deltaic environments tephra material is far less abundant and has been subjected to syn-depositional sorting.

Remarkably, in hardly any of the several studies on the distal AV-tephra (from the EU5 phase) at locations further northwest, in Lazio and Tuscany (e.g. Lake Albano and Lake Nemi, Chondrogianni et al., 1996; Lago di Mezzano, Ramrath et al., 1999a, 1999b; Sadori, 2018; Lago di Accesa, Magny et al., 2007), information is provided on the grain size distribution and more than an extremely concise description of its components. An exception is formed by Ramrath et al. (1999a), who describe the AV-layer in the Lago di Mezzano as a 'crystal tuff with pumice, consisting of crystals with a grain size of ca. 50 μm and composed of sanidine and biotite. Leucite, nepheline, hornblende, titanaugite and rare olivine are also present. The rare glass particles are brown and up to 40 μm in diameter'. Though further fining with increasing distance is evident, given the scarcity of data longer distance trends in grain size distribution and composition of the distal AV-tephra remain uncertain.

5.4. Spatial variation of the AV-layer

As already described in Section 4.1, the AV-layer was widely encountered in both the Agro Pontino and Fondi basin, wherever contemporary environmental conditions were suited for its preservation and it occurred at such depth that it was not disturbed by recent soil labour (i.e. mostly deeper than 50 cm below the ground surface). At local scale, considerable differences exist in its spatial continuity that ranges from rather discontinuous in marshes and fluvio-deltaic environments, to virtually continuous in the highly calcareous lakes.

In marshy environments, the tephra was deposited on a dense vegetation that could be reconstructed on the basis of the palaeoecological data as a reed swamp (Doorenbosch and Field, 2019). This most probably also held for fluvio-deltaic environments. Such vegetation did not exist in the highly calcareous lakes and truly anoxic swamps, where additionally bioturbation most likely was of very minor importance. The interception and redistribution of the tephra by vegetation explains the observed marked differences in the continuity of the layer, a phenomenon that has been extensively described in studies of recent tephra falls (e.g. Cutler et al., 2016; Dugmore et al., 2018). Thus, in gyttjas and truly anoxic clays the tephra layer could be readily traced and followed over larger distances, a typical example of which was encountered at Mezzaluna (site 405), where it could be very easily followed as a continuous layer over hundreds of metres. In peats, the AV-layer was often discontinuous and several corings were needed to establish its occurrence. Typical examples are the tephra layers (both AV and Astroni tephra) at Femmina Morta (site 197) and Tumolillo (site 1005) where series of corings had to be performed to identify and sample these layers..

5.5. Comparison of the Agro Pontino-Fondi basin record with other Central Italian records

Our tephrochronological record can be compared with those from other locations in Central Italy. A first example is the study by Margaritelli et al. (2016) and Di Rita et al. (2018) of cores from the Gulf of Gaeta. Though their coring site was situated in between the Somma-Vesuvius and our area of study, and thus distal tephra from the Avellino eruption must have reached the Gulf of Gaeta in significant quantities, they did not find this tephra, nor any trace of the AP2 eruption. However, tephra from the Astroni 3 eruption and tephra that these authors identified as originating from the Capo Miseno eruption (3.7–5.1 ka BP) were found. Remarkably, Bellotti et al. (2016) who studied the Holocene sediments in the very nearby Garigliano delta plain regularly observed a distinct pumice layer, which they identified as the Avellino pumice layer based on the ^{14}C chronology of the cores studied, but no other tephra layers from the Campi Flegrei (Capo Miseno) or

Somma-Vesuvius. They report older pumice layers (>7000 cal BP) as due to Roccamonfina volcanic activity, based on geochemical analyses, but do not report results from these analyses. The study by Jouannic et al. (2013) on the Maccarese lagoon in the Tiber delta concerns a single core in deltaic sediments in which four distal tephra were found. These include the Astroni eruption and earlier eruptions. Here too, no distal tephra from the Avellino and the AP2 eruptions was encountered. Striking is that Avellino tephra has been found in all cores in lacustrine sediments further North: in the Lago di Albano (Chondrogianni et al., 1996), Lago di Mezzano (Ramrath et al., 1999b), and Lago di Accesa (Magny et al.,2007).

In our area of study, we found the AV-tephra layer wherever appropriate sedimentary environments occurred. This further evidences the importance of tephra from the EU5 eruptive phase of the Avellino eruption as tephrochronological marker for the Tyrrhenian coastal region of Central Italy and for the period concerned. That tephrochronological archives may be incomplete is well-known, even if these are from environments in which hiatuses are unlikely to occur, such as crater lakes and deep marine environments. However, our results indicate that if the AV-tephra layer is absent in a potentially suitable sediment archive from the Tyrrhenian coastal area of Southern Lazio and adjacent Campania, this is a contra-indication for continuity in its sediment record and that attention needs to be paid to its absence rather than assuming such continuity, such as in case of the Gulf of Gaeta and Maccarese cores.

5.6. Volcanological implications

Two of the three tephra layers that we found in the two coastal basins studied are ultra-distal facies of pyroclastic density current (PDCs) deposits: the AV and the presumed Astroni 6 tephra. The AV-tephra is related to the EU5 unit, which was generated by phreatomagmatic explosions during the final phases of this eruption. The associated PDCs flowed towards the northwest and reached distances of at least 25 km from a vent located in the western slopes of the Somma-Vesuvius. As discussed in previous studies (e.g. Sulpizio et al., 2008), during emplacement of the EU5 unit no powerful sustained columns were generated. The ash particles were elutriated from the currents and transported by atmospheric winds towards the northwest. These particles were deposited by fallout over a large area (Sulpizio et al., 2014) and their regular grain-size distribution, fining with increasing distance from the vent, supports this emplacement mechanism. The transport of the particles by atmospheric winds can explain the different dispersal direction of EU5 with respect to the units generated by the main eruptive columns, which dispersed their products towards the northeast, pushed by tropospheric winds. In terms of impact on vegetation, humans and anthropic structures it is very important to take into account that with this kind of event the area affected can be very large.

The same phenomenon can explain the distribution of the Astroni 6 unit towards the north. Following Costa et al. (2009), during the initial phase of the Astroni 6 event a 14 km high Plinian column was generated with dispersal of its products (pumice lapilli) towards the east, while the overlying massive ash layers were widely spread over a large part of the central-northern Campanian Plain, in many cases covering archaeological remains (Marzocchella, 1998; Di Vito et al., 1999; Isaia et al., 2004). The absence of a preferential distribution of the ash suggests its correlation with the PDCs that followed the Plinian phase and in particular with an effective elutriation of the ash from the currents distributed radially around the vent and its long distance transport by atmospheric winds.

The AP2 eruption was fed by low eruption columns and was classified as sub-Plinian by Cioni et al. (2008). Its proximal products show a preferential distribution of the coarse material towards the eastern quadrants of the Somma-Vesuvius. During the eruption a long lasting ash emission occurred generating a large amount of ash dispersed in the atmosphere (Andronico and Cioni, 2002). This ash was transported by atmospheric winds over large distances. The finding of a thin ash layer from this eruption both in Calabria (Sevink et al., 2019) and in southern Lazio opens new perspectives for tephrostratigraphic reconstructions in central-southern Italy.

Together, the results for these three distal tephra demonstrate that even low-magnitude eruptions or phases of the Plinian events may lead to widespread distribution of tephra, far beyond the proximal areas. Most studies of volcanic hazards posed by the Campanian volcanoes tend to concentrate on proximal areas (e.g. Andronico and Cioni, 2002; Cioni et al., 2008). Quantities of erupted pyroclastics are often based on estimates for proximal deposits and do not include the truly distal tephra. In the case of the EU5 event, a rough estimate can be based on known occurrences of the distal EU5 layer to the northwest of the vent and a realistic mean thickness of 2 cm. This already leads to an estimated c. 0.2 km^3 of ejected tephra for the Tyrrhenian coastal area, while the total volume of proximal tephra (10 cm isopach) that was erupted during the full AV-eruption (EU1–5) has been estimated at c. 1.3 km^3 by Zanchetta et al. (2011). Our results thus are in support of the study by Sulpizio et al. (2014), who stressed the hazards posed by such events to truly distal areas.

6. Conclusions

Towards the end of the third millennium BC postglacial sea level rise declined. Under these changing conditions, along the Tyrrhenian coast of Southern Lazio long-shore sediment transport could lead to closure of beach ridge systems, inducing the development of freshwater lagoons. In the Agro Pontino and the Fondi basin, this created optimal conditions for preservation of distal tephra from Campanian volcanoes (Somma-Vesuvius and Campi Flegrei) falling into lagoons and lakes, and on associated marshy lowlands. The first of these was an Astroni eruption (most probably the Astroni 6 eruption), of which tephra was only encountered in the Fondi basin, followed by the much more massive arrival of tephra from the Avellino pumice eruption (EU5) and ultimately by a minor volume of tephra from the AP2 eruption, around 1700 cal BC, which was traced in the southern Agro Pontino. Younger tephra falls were never encountered as recognizable layers in the many hundreds of corings executed, most probably because of a combination of modern intensive soil labour destroying any eventually existing tephra layer, a limited later (post c. 1700 cal BC) accumulation of peat and clastic sediment, and lesser suited conditions for tephra preservation (notably soil erosion and massive colluviation) from the Early Iron Age onward. Moreover, ash plumes from later eruptions may well have had a more eastern or southern direction.

The three distal tephra layers were identified based on: i. their sedimentological features and stratigraphic position; ii. the chemical composition of their volcanic glass; iii. The age constrained by radiocarbon dating. The AV-layer exhibited distinct fining with increasing distance from the volcano, but has markedly uniform macro characteristics, and a rather invariable chemical and mineralogical composition. It constitutes a readily identifiable, major marker bed in these coastal basins, allowing for detailed palaeogeographical reconstructions, and testifies to the magnitude and direction of the EU5 tephra plume, which reached as far as the Lago di Accesa in Central Tuscany. Tephra from the AP2 eruption and the Astroni 6 eruption, though both of lesser magnitude than the Plinian events, must also have spread over the whole of the Tyrrhenian coastal area of Central Italy, though in lesser amounts. This identification has important implications for the impact of these relatively low-magnitude eruptions, both in terms of emitted volume and areal distribution. Moreover, the results underscore the need to include such minor events in volcanic hazard analyses and to extend these to more distal areas.

This study confirms the need to use multiple corings for obtaining a complete tephrostratigraphic record for these Mediterranean coastal and deltaic areas, and for the recognition of eventual hiatuses in the sediment archives studied. Only in truly tranquil lacustrine to anoxic paludal environments we encountered more or less continuous tephra layers, but sediments from such environments unfortunately rarely

hold plant macro remains that are suited for radiocarbon dating. It is only through an extensive coring program and study of a series of cores in a range of sedimentary environments in the southern Lazial coastal basins that we were able to obtain such complete stratigraphy for the time window comprised between c. 2500 and c. 1000 BCE. In Central Italy this period roughly corresponds to the Central Italian Bronze Age.

Data sets and other Supplementary material can be found at doi:10.17632/94xcsy9b2g.1, an open-source online data repository hosted at Mendeley Data. Supplementary data to this article can be found online at https://doi.org/10.1016/j.jvolgeores.2020.107041.

CRediT authorship contribution statement

Jan Sevink: Conceptualization, Methodology, Validation, Investigation, Resources, Writing - original draft, Writing - review & editing, Supervision, Project administration. **Wouter van Gorp:** Investigation, Resources, Writing - review & editing. **Mauro A. Di Vito:** Methodology, Validation, Investigation, Resources, Writing - review & editing. **Ilenia Arienzo:** Methodology, Validation, Investigation, Resources, Writing - review & editing.

Declaration of competing interest

The authors declare that they have no known competing financial interests or personal relationships that could have appeared to influence the work reported in this paper.

Acknowledgements

The authors sincerely thank Roberto Sulpizio and an anonymous reviewer for their suggestions and constructive comments that improved the quality of the manuscript. The extensive coring and sampling program, which formed the basis for this research, had not been possible without the aid of the other AV-project members: Luca Alessandri, Mike Field and Marieke Doorenbosch. In the lab, we were supported by Mike Field and Erica van Hees, both from Leiden University, with the selection and identification of plant macro remains for radiocarbon dating. We thank Corrie Bakels, Mike Field, and Marieke Doorenbosch for their helpful comments. RCE at Amersfoort produced the thin sections, while facilities for grain size analysis were provided by the Vrije Universiteit Amsterdam with the support of Maarten Prins, Martine Hagen, and Unze van Buuren. Hans van der Plicht and Luca Alessandri aided with the Bayesian analysis of the radiocarbon data and interpretation of the ^{14}C datings. Manuela Nazzari and Piergiorgio Scarlato are thanked for their assistance during the electron microprobe analyses at Rome. Thanks are also due to Anna Maiello and Enrico Vertechi for their support during purchase of the material necessary for the laboratory analyses at INGV, OV.

Funding

This work was supported by The Netherlands Organisation for Scientific Research (NWO), Free Competition grant 360-61-060. The INGV, OV laboratories were financially supported by the EPOS Research Infrastructure through the contribution of the Italian Ministry of University and Research (MUR). The research by the INGV also received financial support from the Presidenza del Consiglio dei Ministri e Dipartimento della Protezione Civile DPC-INGV project B2 WP 2 task 1.

References

Alessandri, L., 2019. The early and Middle Bronze Age (1/2) in South and central Tyrrhenian Italy and their connections with the Avellino eruption: an overview. Quat. Int. 499, 161–185. https://doi.org/10.1016/j.quaint.2018.08.002.

Andronico, D., Cioni, R., 2002. Contrasting styles of Mount Vesuvius activity in the period between the Avellino and Pompeii Plinian eruptions, and some implications for assessment of future hazards. Bull. Volcanol. 64 (6), 372–391. https://doi.org/10.1007/s00445-002-0215-4.

Arienzo, I., Moretti, R., Civetta, L., Orsi, G., Papale, P., 2010. The feeding system of Agnano-Monte Spina eruption (Campi Flegrei, Italy): dragging the past into the present activity and future scenarios. Chem. Geology 270 (1–4), 135–147. https://doi.org/10.1016/j.chemgeo.2009.11.012.

Arienzo, I., D'Antonio, M., Di Renzo, V., Tonarini, S., Minolfi, G., Orsi, G., Carandente, A., Belviso, P., Civetta, L., 2015. Isotopic microanalysis sheds light on the magmatic endmembers feeding volcanic eruptions: the Astroni 6 case study (Campi Flegrei, Italy). J. Volcanol. Geotherm. Res. 304, 24–37. https://doi.org/10.1016/j.jvolgeores.2015.08.003.

Arienzo, I., Mazzeo, F.C., Moretti, R., Cavallo, A., D'Antonio, M., 2016. Open-system magma evolution and fluid transfer at Campi Flegrei caldera (Southern Italy) during the past 5 ka as revealed by geochemical and isotopic data: the archetype of Nisida eruption. Chem. Geol. 427, 109–124. https://doi.org/10.1016/j.chemgeo.2016.02.007.

Attema, P., 2017. Sedimentation as geomorphological bias and indicator of agricultural (un) sustainability in the study of the coastal plains of South and Central Italy in antiquity. J. Archaeol. Sci. Rep. 15, 459–469. https://doi.org/10.1016/j.jasrep.2016.07.024.

Bakels, C., Sevink, J., Kuijper, W., Kamermans, H., 2015. The Agro Pontino Region, Refuge after the Early Bronze Age Avellino Eruption of Mount Vesuvius, Italy? Analecta Praehist. Leidensia. vol. 45. Leiden University, pp. 55–68. https://hdl.handle.net/11245/1.491854.

Bellotti, P., Calderoni, G., Dall'Aglio, P.L., D'Amico, C., Davoli, L., Di Bella, L., D'Orefice, M., Esu, D., Ferrari, K., Bandini Mazzanti, M., Mercuri, A.M., Tarragoni, C., Torri, P., 2016. Middle-to late-Holocene environmental changes in the Garigliano delta plain (Central Italy): which landscape witnessed the development of the Minturnae Roman colony? The Holocene 26 (9), 1457–1471. https://doi.org/10.1177/0959683616640055.

Blockley, S.P.E., Bronk Ramsey, C., Pyle, D.M., 2008. Improved age modelling and high-precision age estimates of late Quaternary tephras, for accurate palaeoclimate reconstruction. J. Volcanol. Geotherm. Res. 177, 251–262. https://doi.org/10.1016/j.jvolgeores.2007.10.015.

Bronk Ramsey, C., 2017. OxCal Program, Version 4.3.

Chondrogianni, C., Ariztegui, D., Guilizzoni, P., Lami, A., 1996. Lakes Albano and Nemi (central Italy): an overview. Mem.-Istituto Italiano Idrobiol. 55, 17–22.

Cioni, R., Bertagnini, A., Santacroce, R., Andronico, D., 2008. Explosive activity and eruption scenarios at Somma-Vesuvius (Italy): towards a new classification scheme. J. Volcanol. Geotherm. Res. 178, 331–346. https://doi.org/10.1016/j.jvolgeores.2008.04.024.

Civetta, L., Galati, R., Santacroce, R., 1991. Magma mixing and convective compositional layering within the Vesuvius magma chamber. Bull. Volcanol. 53, 287–300. https://doi.org/10.1007/BF00414525.

Costa, A., Dell'Erba, F., Di Vito, M., Isaia, R., Macedonio, G., Orsi, G., Pfeiffer, T., 2009. Tephra fallout hazard assessment at the Campi Flegrei caldera (Italy). Bull. Volcanol. 71, 259–273. https://doi.org/10.1007/s00445-008-0220-3.

Cutler, N.A., Shears, O.M., Streeter, R.T., Dugmore, A.J., 2016. Impact of small-scale vegetation structure on tephra layer preservation. Sci. Reports 6, 37260. https://doi.org/10.1038/srep37260.

D'Antonio, M., Tonarini, S., Arienzo, I., Civetta, L., Di Renzo, V., 2007. Components and processes in the magma genesis of the Phlegrean Volcanic District, southern Italy. Geol. Soc. Amer., Spec. Paper 418, 203–220. https://doi.org/10.1130/2007.2418(10).

D'Antonio, M., Tonarini, S., Arienzo, I., Civetta, L., Dallai, L., Moretti, R., Orsi, G., Andria, M., Trecalli, A., 2013. Mantle and crustal processes in the magmatism of the Campania region: inferences from mineralogy, geochemistry, and Sr–Nd–O isotopes of young hybrid volcanics of the Ischia island (South Italy). Contrib. Mineral. Petrol. 165, 1173–1194. https://doi.org/10.1007/s00410-013-0853-x.

Dent, D.L., 1986. Acid Sulphate Soils: A Baseline for Research and Development. No. 39. ILRI, Wageningen, The Netherlands (204 pp).

Di Renzo, V., Arienzo, I., Civetta, L., D'Antonio, M., Tonarini, S., Di Vito, M.A., Orsi, G., 2011. The magmatic feeding system of the Campi Flegrei caldera: architecture and temporal evolution. Chem. Geol. 281, 227–241. https://doi.org/10.1016/j.chemgeo.2010.12.010.

Di Rita, F., Lirer, F., Bonomo, S., Cascella, A., Ferraro, L., Florindo, F., Insinga, D.D., Lurcock, P.C., Margaritelli, G., Petrosino, P., Rettori, R., Vallefuaco, M., Magri, D., 2018. Late Holocene forest dynamics in the Gulf of Gaeta (central Mediterranean) in relation to NAO variability and human impact. Quat. Sci. Rev. 179, 137–152. https://doi.org/10.1016/j.quascirev.2017.11.012.

Di Vito, M.A., Isaia, R., Orsi, G., Southon, J., de Vita, S., D'Antonio, M., Pappalardo, L., Piochi, M., 1999. Volcanism and deformation since 12,000 years at the Campi Flegrei caldera (Italy). J. Volcanol. Geotherm. Res. 91, 221–246. https://doi.org/10.1016/S0377-0273(99)00037-2.

Di Vito, M.A., Castaldo, N., de Vita, S., Bishop, J., Vecchio, G., 2013. Human colonization and volcanic activity in the eastern Campania Plain (Italy) between the Eneolithic and Late Roman periods. Quat. Int. 303, 132–141. https://doi.org/10.1016/j.quaint.2013.01.001.

Doorenbosch, M., Field, M.H., 2019. A Bronze Age palaeoenvironmental reconstruction from the Fondi basin, southern Lazio, central Italy. Quat. Int. 499, 221–230. https://doi.org/10.1016/j.quaint.2018.03.022.

Dugmore, A., Streeter, R., Cutler, N., 2018. The role of vegetation cover and slope angle in tephra layer preservation and implications for quaternary tephrostratigraphy. Palaeogeogr., Palaeoclim., Palaeoecol. 489, 105–116. https://doi.org/10.1016/j.palaeo.2017.10.002.

Feiken, H., 2014. Dealing with Biases: Three Geo-archaeological Approaches to the Hidden Landscapes of Italy. vol. 26. Barkhuis, The Netherlands.

Feiken, H., Tol, G.W., Van Leusen, P.M., Anastasia, C., 2012. Reconstructing a Bronze Age hidden landscape: geoarchaeological research at Tratturo Caniò (Italy, 2009). Palaeohistoria 109–159.

Giaccio, B., Messina, P., Sposato, A., Voltaggio, M., Zanchetta, G., Galadini, F., Gpori, S., Santacroce, R., 2009. Tephra layers from Holocene lake sediments of the Sulmona Basin, central Italy: implications for volcanic activity in Peninsular Italy and tephrostratigraphy in the central Mediterranean area. Quat. Sci. Rev. 28 (25–26), 2710–2733. https://doi.org/10.1016/j.quascirev.2009.06.009.

Insinga, D., Calvert, A.T., Lanphere, M.A., Morra, V., Perrotta, A., Sacchi, M., Scarpati, C., Saburomaru, J., Fedele, L., 2006. The Late-Holocene evolution of the Miseno area (southwestern Campi Flegrei) as inferred by stratigraphy, petrochemistry and $^{40}Ar/^{39}Ar$ geochronology. In: De Vivo, B. (Ed.), Volcanism in the Campania Plain: Vesuvius, Campi Flegrei and Ignimbrites. Elsevier, pp. 97–124.

Iovine, R.S., Fedele, L., Mazzeo, F.C., Arienzo, I., Cavallo, A., Wörner, G., Orsi, G., Civetta, L., D'Antonio, M., 2017a. Timescales of magmatic processes prior to the ~4.7 ka Agnano-Monte Spina eruption (Campi Flegrei caldera, Southern Italy) based on diffusion chronometry from sanidine phenocrysts. Bull. Volcanol. 79 (2), 18. https://doi.org/10.1007/s00445-017-1101-4.

Iovine, R.S., Mazzeo, F.C., Arienzo, I., D'Antonio, M., Wörner, G., Civetta, L., Pastore, Z., Orsi, G., 2017b. Source and magmatic evolution inferred from geochemical and Sr-O-isotope data on hybrid lavas of Arso, the last eruption at Ischia island (Italy; 1302 AD). J. Volcanol. Geotherm. Res. 331, 1–15. https://doi.org/10.1016/j.jvolgeores.2016.08.008.

Iovine, R.S., Mazzeo, F.C., Wörner, G., Pelullo, C., Cirillo, G., Arienzo, I., Pack, A., D'Antonio, M., 2018. Coupled $\delta^{18}O$-$\delta^{17}O$ and $^{87}Sr/^{86}Sr$ isotope compositions suggest a radiogenic and ^{18}O-enriched magma source for Neapolitan volcanoes (Southern Italy). Lithos 316-317, 199–211. https://doi.org/10.1016/j.lithos.2018.07.009.

Isaia, R., D'Antonio, M., Dell'Erba, F., Di Vito, M.A., Orsi, G., 2004. The Astroni volcano: the only example of close eruptions within the same vent area during the recent history of the Campi Flegrei caldera (Italy). J. Volcanol. Geotherm. Res. 133, 171–192. https://doi.org/10.1016/S0377-0273(03)00397-4.

Jouannic, G., Gillot, P.Y., Goiran, J.P., Lefevre, J.C., Siani, G., Salomon, F., Arnoldus-Huyzendveld, A., 2013. Tephrochronological study in the Maccarese Lagoon (near Rome, Italy): identification of Holocene tephra layers. Quat., Rev. Assoc. Franc. Et. Quat. 24 (1), 65–74.

Jung, R., 2017. Chronological problems of the Middle Bronze age in Southern Italy. In: Lachenal, T., Mordant, J., Nicolas, T., Véber, C. (Eds.), Le Bronze moyen et l'origine du Bronze final en Europe occidentale (XVIIe–XIIIe siècle av. J.-C.). Colloque international de l'APRAB, Strasbourg, 17 au 20 juin 2014. Mém. Archéol. Grand-Est 1, pp. 623–642.

Lambeck, K., Antonioli, F., Anzidei, M., Ferranti, L., Leoni, G., Scicchitano, G., Silenzi, S., 2011. Sea level change along the Italian coast during the Holocene and projections for the future. Quat. Int. 232 (1), 250–257. https://doi.org/10.1016/j.quaint.2010.04.026.

Magny, M., De Beaulieu, J.L., Drescher-Schneider, R., Vannière, B., Walter-Simonnet, A.V., Miras, Y., Millet, L., Bossuet, G., Peyron, O., Brugiapaglia, E., Leroux, A., 2007. Holocene climate changes in the central Mediterranean as recorded by lake-level fluctuations at Lake Accesa (Tuscany, Italy). Quat. Sci. Rev. 26 (13–14), 1736–1758. https://doi.org/10.1016/j.quascirev.2007.04.014.

Margaritelli, G., Vallefuoco, M., Di Rita, F., Capotondi, L., Bellucci, L.G., Insinga, D.D. Petrosino,P., Bonomoa, S., Cacho, I., Cascella, A., Ferraroa, L., Florindo, F., Lubritto, C., Lurcock, P.C., Magri, D., Pelosi, N., Rettori, R., Lirer, F., 2016. Marine response to climate changes during the last five millennia in the central Mediterranean Sea. Glob. Planetary Change 142, 53–72. doi:https://doi.org/10.1016/j.gloplacha.2016.04.007.

Marzocchella, A., 1998. Tutela Archeologica e Preistoria nella Pianura Campana. In: Guzzo, P.G., Peroni, R. (Eds.), Archeologia e Vulcanologia in Campania. Arte Tipografica, Napoli, pp. 97–133.

Orsi, G., Di Vito, M.A., Selva, J., Marzocchi, W., 2009. Long-term forecast of eruption style and size at Campi Flegrei caldera (Italy). Earth Planet. Sci. Lett. 287, 265–276. https://doi.org/10.1016/j.epsl.2009.08.013.

Petrini, R., Forte, C., Orsi, G., Piochi, M., Pinzino, C., Pedrazzi, G., 2001. Influence of magma dynamics on melt structure: spectroscopic studies on volcanic glasses from the Cretaio Tephra of Ischia (Italy). Contrib. Mineral. Petrol. 140, 532–542. https://doi.org/10.1007/s004100000209.

Ramrath, A., Nowaczyk, N.R., Negendank, J.F., 1999a. Sedimentological evidence for environmental changes since 34,000 years BP from Lago di Mezzano, central Italy. J. Paleolimnol. 21 (4), 423–435. https://doi.org/10.1016/S0277-3791(99)00009-8.

Ramrath, A., Zolitschka, B., Wulf, S., Negendank, J.F., 1999b. Late Pleistocene climatic variations as recorded in two Italian maar lakes (Lago di Mezzano, Lago Grande di Monticchio). Quat. Sci. Rev. 18 (7), 977–992. https://doi.org/10.1016/S0277-3791(99)00009-8.

Sadori, L., 2018. The Lateglacial and Holocene vegetation and climate history of Lago di Mezzano (central Italy). Quat. Sci. Rev. 202, 30–44. https://doi.org/10.1016/j.quascirev.2018.09.004.

Santacroce, R., Cioni, R., Marianelli, P., Sbrana, A., Sulpizio, R., Zanchetta, G., Donahue, D.J., Joron, J.L., 2008. Age and whole rock-glass compositions of proximal pyroclastics from the major explosive eruptions of Somma-Vesuvius: a review as a tool for distal tephrostratigraphy. J. Volcanol. Geotherm. Res. 177, 1–18. https://doi.org/10.1016/j.jvolgeores.2008.06.009.

Sevink, J., 2020. Burnt clay or terra bruciata in coastal basins of Southern Lazio, Italy: evidence for prehistoric ignicoltura or resulting from drainage of Holocene pyritic sediments? J. Archaeol. Sci. Rep. 32. https://doi.org/10.1016/j.jasrep.2020.102432.

Sevink, J., Vos, P., Westerhoff, W.E., Stierman, A., Kamermans, H., 1982. A sequence of marine terraces near Latina (Agro Pontino, Central Italy). Catena 9 (3/4), 361–378. https://doi.org/10.1016/0341-8162(82)90010-8.

Sevink, J., Remmelzwaal, A., Spaargaren, O.C., 1984. The soils of Southern Lazio and adjacent Campania. Publ. Fys. Geogr. Lab. UvA, nr. 38, p. 140.

Sevink, J., van Bergen, M.J., van der Plicht, J., Feiken, H., Anastasia, C., Huizinga, A., 2011. Robust date for the Bronze age Avellino eruption (Somma-Vesuvius): 3945 ± 10 calBP (1995 ± 10 calBC)Quat. Sci. Rev. 30, 1035–1046. https://doi.org/10.1016/j.quascirev.2011.02.001.

Sevink, J., Van der Plicht, J., Feiken, H., Van Leusen, P.M., Bakels, C.C., 2013. The Holocene of the Agro Pontino graben: recent advances in its palaeogeography, palaeoecology, and tephrostratigraphy. Quat. Int. 303, 153–162. https://doi.org/10.1016/j.quaint.2013.01.006.

Sevink, J., di Vito, M.A., Piochi, M., Mormone, A., Bakels, C.C., Van Gorp, W., 2018. A rare Mid-Würmian lithoid tuff in the Agro Pontino graben (Southern Lazio, Italy) and its identification as an Albano 5-7 related distal tephra deposit (41-36 kaBP): characteristics, provenance and palaeogeographical implications. Ann. Geophys. 61 (1), 1–15. https://doi.org/10.4401/ag-7574.

Sevink, J., Bakels, C., Attema, P., Di Vito, M.A., Arienzo, I., 2019. Holocene vegetation record of upland northern Calabria, Italy: environmental change and human impact. The Holocene 29 (4), 633–647. https://doi.org/10.1177/0959683618824695.

Sevink, J., Bakels, C.C., Van Hall, R.L., Dee, M.W., 2020. Radiocarbon dating distal tephra from the Early Bronze Age Avellino eruption (EU 5) in the coastal basins of southern Lazio (Italy): uncertainties, results, and implications for dating distal tephra. Submitted. Quat. Geochronol.

Smith, V.C., Isaia, R., Pearce, N.J.G., 2011. Tephrostratigraphy and glass compositions of post-15 kyr Campi Flegrei eruptions: implications for eruption history and chronostratigraphic markers. Quat. Sci. Rev. 30 (25–26), 3638–3660. https://doi.org/10.1016/j.quascirev.2011.07.012.

Sulpizio, R., Bonasia, R., Dellino, P., Di Vito, M.A., La Volpe, L., Mele, D., Zanchetta, G., Sadori, L., 2008. Discriminating the long distance dispersal of fine ash from sustained columns or near ground ash clouds: the example of the Pomici di Avellino eruption (Somma-Vesuvius, Italy). J. Volcanol. Geotherm. Res. 177 (1), 263–276. https://doi.org/10.1016/j.jvolgeores.2007.11.012.

Sulpizio, R., Cioni, R., Di Vito, M.A., Mele, D., Bonasia, R., Dellino, P., 2010a. The Pomici di Avellino eruption of Somma-Vesuvius (3.9 ka BP). Part I: stratigraphy, compositional variability and eruptive dynamics. Bull. Volcanol. 72 (5), 539–558. https://doi.org/10.1007/s00445-009-0339-x.

Sulpizio, R., Bonasia, R., Dellino, P., Mele, D., Di Vito, M.A., La Volpe, L., 2010b. The Pomici di Avellino eruption of Somma–Vesuvius (3.9 ka BP). Part II: sedimentology and physical volcanology of pyroclastic density current deposits. Bull. Volcanol. 72 (5), 559–577. https://doi.org/10.1007/s00445-009-0340-4.

Sulpizio, R., Welden, A.V., Caron, B., Zanchetta, G., 2010c. The Holocene tephrostratigraphic record of Lake Shkodra (Albania and Montenegro). J. Quat. Sci. 25 (5), 633–650. https://doi.org/10.1002/jqs.1334.

Sulpizio, R., Zanchetta, G., Caron, B., Dellino, P.F., Mele, D., Giaccio, B., Insinga, D., Paterne, M., Siani, G., Costa, A., Macedonio, G., Santacroce, R., 2014. Volcanic ash hazard in the Central Mediterranean assessed from geological data. Bull. Volcanol. 76, 866. https://doi.org/10.1007/s00445-014-0866-y.

Tonarini, S., D'Antonio, M., Di Vito, M.A., Orsi, G., Carandente, A., 2009. Geochemical and B-Sr-Nd isotopic evidence for mingling and mixing processes in the magmatic system that fed the Astroni volcano (4.1–3.8 ka) within the Campi Flegrei caldera (southern Italy). Lithos 107, 135–151. https://doi.org/10.1016/j.lithos.2008.09.012.

Vacchi, M., Marriner, N., Morhange, C., Spada, G., Fontana, A., Rovere, A., 2016. Multiproxy assessment of Holocene relative sea-level changes in the western Mediterranean: sea-level variability and improvements in the definition of the isostatic signal. Earth-Sci. Rev. 155, 172–197. https://doi.org/10.1016/j.earscirev.2016.02.002.

Van Gorp, W., Sevink, J., 2019. Distal deposits of the Avellino eruption as a marker for the detailed reconstruction of the Early Bronze Age depositional environment in the Agro Pontino and Fondi Basin (Lazio, Italy). Quat. Int. 499, 245–257. https://doi.org/10.1016/j.quaint.2018.03.017.

van Gorp, W., Sevink, J., van Leusen, P.M., 2020. Post-depositional subsidence of the Avellino tephra marker bed in the Pontine plain (Lazio, Italy): implications for Early Bronze Age palaeogeographical, water level and relative sea level reconstruction. Catena 194, 104770. https://doi.org/10.1016/j.catena.2020.104770.

Van Joolen, E., 2003. Archaeological Land Evaluation. A Reconstruction of the Suitability of Ancient Landscapes for Various Land Uses in Italy Focused on the First Millennium BC. Groningen.

Wulf, S., Kraml, M., Brauer, A., Keller, J., Negendank, J.F., 2004. Tephrochronology of the 100 ka lacustrine sediment record of Lago Grande di Monticchio (southern Italy). Quat. Int. 122 (1), 7–30. https://doi.org/10.1016/j.quaint.2004.01.028.

Zanchetta, G., Sulpizio, R., Roberts, N., Cioni, R., Eastwood, W.J., Siani, G., Caron, B., Paterne, M., Santacroce, R., 2011. Tephrostratigraphy, chronology and climatic events of the Mediterranean basin during the Holocene: an overview. The Holocene 21, 33–52. https://doi.org/10.1177/0959683610377531.